

Low speed brushless PMSM for for in-wheel application

Damia-2 application status report



Avo Reinap

Division of Industrial Electrical Engineering and Automation
Faculty of Engineering, Lund University

Low speed brushless PMSM for in-wheel application

This is a reviewing document (a progress report on Damia-2) on design and evaluation of an outer rotor surface mounted permanent magnet synchronous machine for in-wheel drive application. The scope and outcomes of the work is summarized as follows:

1. 4 different design generations with the following number of poles (P), slots (S) inner to outer diameter [mm] ratios (“electromagnetically active volume”):
 - a. 22P18S Ø160/270 changed dimensions to Ø120/256,
 - b. 22P18S, 26P27S, 28P21S and 32P27S (Figure 3.6) Ø180/260,
 - c. 28P30S Ø240/310 that uses a balanced modular winding 5 coils per segment,
 - d. 22P22S Ø120/190 that uses two segments with direct cooled wave / laminated windings.
2. Initial focus on distributed concentrated windings, development and realization of wave-windings for electrical machines,
3. Initial focus on SM²C core, later development towards hybrid cores by using core inserts.

The specific outcome to the machine design and manufacturing of the machine has resulted to (incl. Figure 1.1)

1. Systematic scan trough of the **distributed concentrated windings and core material combinations** for the specified size of the machine based on 2D FEA,
2. Comparison of **different stators** as a combination of manufacturing and design concepts,
3. Machine prototyping with the unique approach of **combining molding and integration of stator parts**.

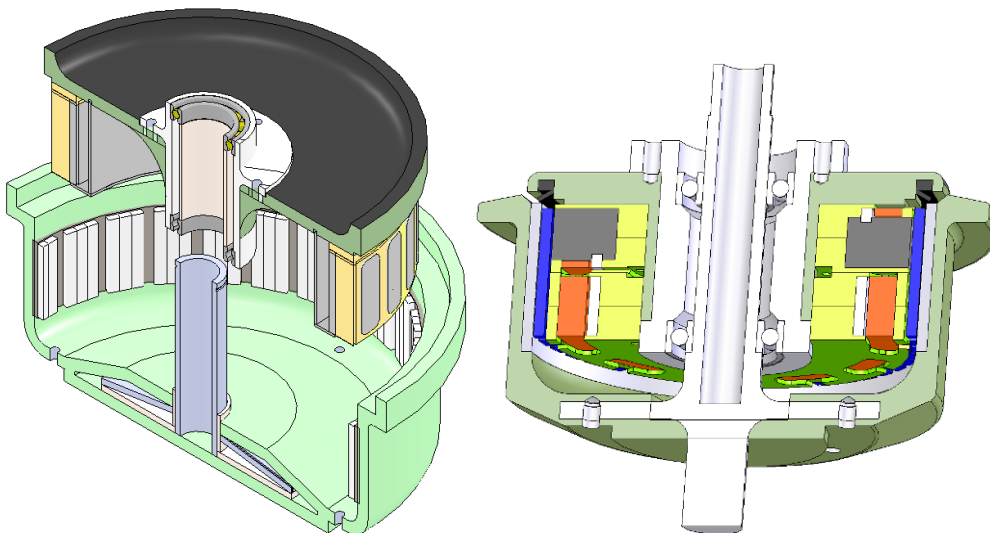


Figure 1.1 Prototyped machines: CAD drawing of W3 and W4

Acknowledgement

The author of the report is grateful for both the funding from the SSF ProViking program and the close cooperation between the university divisions and with the project parties and their members involved in the design and prototype building of in-wheel electric machines / hub motors.

1	Manufacturing, design and target specifications.....	3
1.1	Design-to-Manufacturing interactions.....	3
1.2	Focus areas	3
1.3	Machine topology specification	4
2	Design and practical experience of a medium Ø270 PMSM	6
2.1	Design milestones of W1	7
2.2	Manufacturing experience of W1	10
3	Redesign of W1 resulting W2 and W3.....	12
3.1	Design of a medium Ø260 and large Ø310 PMSM	12
3.2	Selection of pole-to-slot configuration.....	17
3.3	Comparison of baseline designs	18
4	Prototyping and evaluation of a large Ø310 PMSM.....	20
4.1	Short overview.....	20
4.2	Manufactured stators and flux linkage comparison.....	21
4.3	Evaluation process	23
4.4	Remarks for further development.....	32
5	Prototyping and evaluation of a small Ø190 PMSM.....	37
5.1	Mechanical design	37
5.2	Electromagnetic design	39
5.3	Prototyping and evaluation process	44
6	Conclusions and future work	50
	References.....	51

1 Manufacturing, design and target specifications

This chapter provides a more general overview of both the project objectives and hub integrated gearless electric machines - in-wheel motors. What makes the design of hub motors interesting is the fact that if the expected characteristics of the machine or the production technological solutions do not allow the desired goals to be achieved, then the design is also changed. The motto of the design process is simplicity provides progress.

1.1 Design-to-Manufacturing interactions

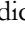
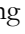
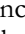
Table 1.1 gives an overview of the main milestones in the design and development of in-wheel machines, indicating whether it is purely theoretical design (proposal or initialization) , design to manufacturing interaction  or prototyping and experimental evaluation . Coil types are indicated by letters: concentrated coil (C), wave coil (W) and laminated coil (L) with an approximate date when the coil type began to be used. The prototype number for the 3rd generation design will be provided at the time the prototype is manufactured. Interactions between manufacturing and design usually occur during technology development and the opposite direction during the design (evaluation) process, where the first evaluation is based on a model.

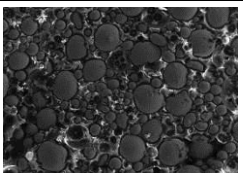

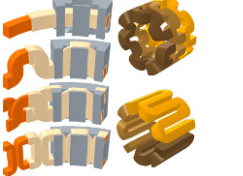

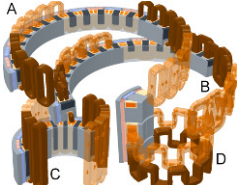
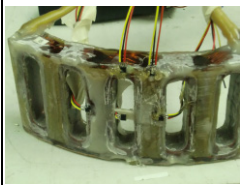
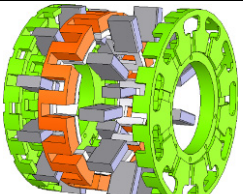
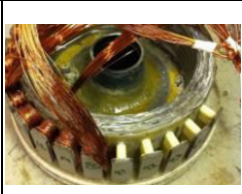
Table 1.1 Technology and design development steps for in-wheel applications with pole (P) slot (S) numbers and diameter ratio (stator inner diameter / rotor outer diameter)

	2008	2009	2010	2011	2012	2013
Competence & technology development						
SM ² C development and characterization						
Development of molding technique & molds						
Development of moldable windings	C	W		L		
Development of combined cores, cooling, etc						
Winding insulation characterization						
Winding production automation						
Prototype realization and evaluation						
Design W1: 22P18S Ø160/270 → 120/256						
Design W2: 22P18S...32P27S Ø180/260						
Design W3: 28P30S Ø240/310				1	2	3 4
Design W4: 22P22S Ø120/190						

1.2 Focus areas

The design and manufacturability of electrical machines for in-wheel vehicular application is one of the main objects in the (DAMIA-2) project where the practical production of the electrical machine components has begun and influenced other designs for other applications. The ultimate goal for the project is to demonstrate the potential of SM²C in machine application with a number of different prototypes where the electrical machines are designed according to application needs and are made of soft magnetic moldable composite. The alternative and innovative production method for the electrical machines, which facilitates a high degree of integration where the injected soft magnetic composite joins the components in the mold to the magnetic core. Consequently, the machine windings are preferably completed and fixed in advance in the mold, and the molding is considered as a single step assembling process. Hence the fields of interests: manufacturability and design is tightly connected, and the good basis of competence and technology development becomes the success in the product realization and development. The overview of the important activities related to focus areas is summarized in Table 1.2:

Table 1.2 Activities and outcomes related to focus areas

SM2C material development and characterization. The magnetic permeability determines torque capability and power losses the efficiency		Development of molding techniques and design of mold characterize the actually achievable material properties and a complexity of the core	
Design of moldable windings focuses on manufacturability and torque capability. A modular concentrated coils and wave-windings are the choices		At least two complete machines and a number of useful tools are prototyped for semi-automated production of moldable windings	
There are considerable amount of analyses behind the designs that consider a various machine configurations, material choices, manufacturing options, etc		Practical realization of machine windings gain a lot of attention that inspires and establishes the origin for the new machine topologies and research	
The challenging part of this project is to provide the best designs that are able to take the potential of SM2C and production method and to fulfill all the application requirements		There are more than 30 prototypes, from small size and experimental study to medium and large machines to meet the application requirements	

1.3 Machine topology specification

The specific features of SM²C core establish number **prospects**:

1. **Stator coils** must be **premade** (performed or pre wound) in order to be molded,
2. Permanent magnet excitation – **permanent magnets** can perfectly magnetize air-core machines, so they are even better for the machines with magnetic core.
3. **High number of poles** means shorter magnetization bath and higher frequency, both these are perfect match for SM²C. The consequence is that with high number of poles and magnets the reluctance forces between the core and the magnets that results as a **high cogging**.
4. Distributed concentrated winding that is grouped per phase so that the build up a **modular winding** (Figure 1.2) is the next natural choice and the challenge for production. It is the simplest to produce a solenoid, and bit more advanced to form the shape to become a chain of solenoids in the modular winding.

Some basic shapes of pre-wound coils are shown in Figure 1.1. The circumferentially distributed wave windings are shown as single layer single turn winding. A double layer or a return path needed to be added to establish a multi-turn winding.



Figure 1.1 Three-phase windings: distributed concentrated (left), circumferentially distributed wave (middle) and axially distributed wave winding (right).

Some examples of concentrated coil arrangements that compose a distributed concentrated and when grouped also a modular winding is shown in Figure 1.2.

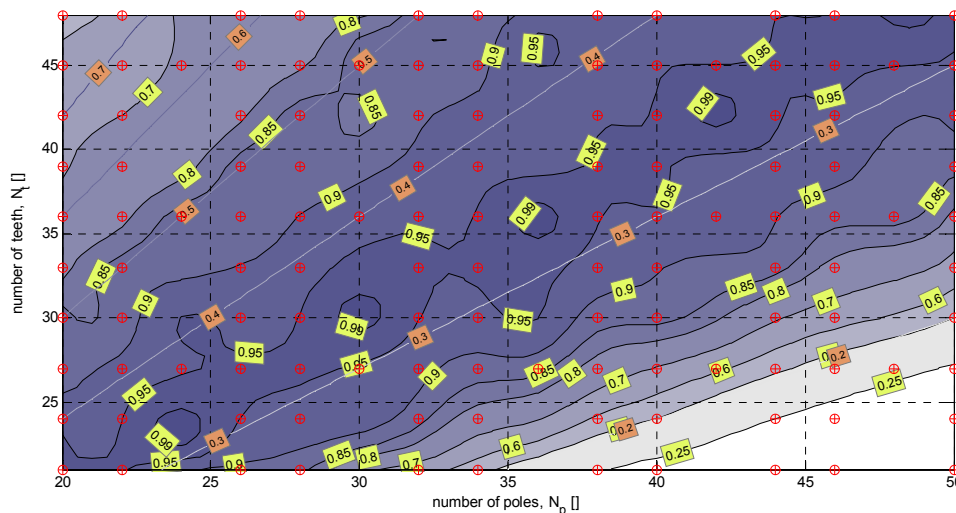


Figure 1.2 Rough dimensioning of a radial flux machine (left) and axial flux machine (right)

Distributed concentrated winding is preferred as it gives a shorter end-turn that can be embedded into a stator core and as in result allows making a more compact machine along the rotating axis. Not all combinations of the number of stator slots (N_s or number of teeth $N_t=N_s$) and the number of rotor slots can establish an electromagnetic coupling and a symmetric three phase system: A figure below indicates the strongest electromagnetic coupling (darker regions with value closer to 1) and the possibility to establish the symmetric three phase system \oplus .

Practical experimentation with a radial flux permanent magnet synchronous machine with SM²C core has shown that:

- a. Cogging torque becomes (much) higher than expected and the reason is the SM²C filling that can cause “dominating pole-pair” so that all the magnets “are presented” when turning the shaft. In this case the cogging became about 15-20% of nominal torque compared to expected value below 1-2%.
- b. SM²C core has a weak shielding ability due to low permeability and this means that the core leaks through the back (and sides!).

2 Design and practical experience of a medium Ø270 PMSM

This is the first serious campaign on designing and manufacturing an outer-rotor permanent magnet synchronous machine with **SM²C stator core** for in-wheel application. The main focus during the design process where not focused on the molding or the impact of the core material properties rather than finding a good compromise layout specification for a radial flux machine and dimensions for the machine parts. According to the specification:

1. The size of the machine is given $D_o=270\text{ mm}$ and $H_{act}=60\text{ mm}$ with the conditions that the end-turns are partly embedded and shall extend beyond the available space in the hub, which is 80 mm ,
2. The application requirement for the performance specified 5.5 kW driving power per wheel at 1200 rpm as the maximum nominal operating speed,
3. The cooling condition is specified 1) natural cooling if it is possible and 2) forced liquid cooling as a supplementary option to extend the design and the performance limits.

This specification is already given in the introductory study where the radial flux machine concept is chosen among axial flux, transversal flux and circumferential flux (torus) machines. This is not the torque capability that demonstrates the clear choice for the radial flux machines rather than several other aspects that are related to mechanical suspension, construction and so on.

For the given active size $V_{act}=2.2\text{ dm}^3$ (assuming $D_i=160\text{ mm}$ for inner diameter) the machine has to produce 44 Nm on the shaft, which is more than 2.8 Nm/Kg by assuming lower equivalent mass density of 7000 kg/m^3 for the machine as the density of the core is less than for conventional cores. The **high specific torque requirement** is something opposite that SM²C machines can naturally/actually provide. In order to compensate the low magnetic permeability of the core

1. The **design** moves in the **direction** of **more coils** and more permanent **magnets**,
2. More coils mean larger **coil area** and also a higher **fill-factor**,
3. The machine construction turns to have relatively **low number of poles** compared to conventional hub motors with the same size,
4. **Concentrated windings** are the only choice to embed the windings and take advantage of flux concentration from tooth-tips to stator teeth,
5. **Modular windings** are preferred among the combinations of distributed concentrated coils vs selection of number of poles,
6. Last, not least, **all available volume is used** for electromechanical energy conversion so that the inner radius is reduced “as much as possible”.

Despite of the design efforts to provide the machine construction, which comes closest to the performance requirements, the proposal is rather **unappealing design**. The reason is that the conventional machines at the similar size and power take more advantage of high number of poles and slimmer construction than the machine with SM²C core in the stator. Regardless of the concern the technical drawings are completed, the prototyping is started, and materials ordered:

1. Vacuumschmelze GmbH provides magnets,
2. Fixture to produce windings are designed and manufactured, one from aluminum another from plastic, and sample winding is provided by industrial production at LTH,
3. First parts of a hub and suspension are provided by Handikappteknik Per Stjärnehag FA.

After the first manufacturing efforts, it becomes clear that the machine has to be changed in order to make it more attractive to produce and take advantage of simple and smart solutions. It is also clear that the design criteria cannot be after high specific torque as the material is not the best choice to provide that. This results a **design paradox** of using material that results **low torque capability** and still trying to apply it to **products** that **require** rather **high torque** at low application speed than low torque at high application speed. From this moment, there is continuous

discussion around **design for manufacturability** rather than providing a complete solution for the application.

1. From manufacturing point of view, it is simple to mold core around a coil and use it at high frequency where the **SM²C** material have **outstanding characteristics**,
2. From design point of view the application **requires torque** from the given space and at the given speed and this is not self-explanatory that the either the speed and size can be easily changed in a **direct drive unit**,
3. The production faces to several new challenges that are no longer self evident: **windings** and **insulation system**,
 - a. machine windings that are able produce torque (without core) is not only a chain of solenoids i.e., easily made – windings can be more **complex**,
 - b. Alternative techniques, processes and experience is required to **arrange** the main insulation,
4. In return, the design process, which mainly becomes an **analysis** and modeling process, starts to seek among the various materials, production processes, and construction layouts and so on in order to **find attractive solutions for production**.

As the consequence, the outcome of the first design proposal for in-wheel application (**W1**) is entered into the **redesign process**, which goal is to **minimize the size** of the machine, provide more attractive layouts for production for the same bounding dimensions and **maintain torque** capability as much as possible.

2.1 Design milestones of W1

After a number of introductory iterations of calculations and analysis the specification of the machine geometry, material and loading becomes for:

1. the distance between the stator and the rotor, the air-gap, is fixed to **$g=1\text{ mm}$** ,
2. the material for the surface mounted permanent magnets (as field weakening and constant power region is not the case for this application) is (initially) selected to be ***N35H***,
3. the current density in the conductor **$J=5\text{A/mm}^2$** ,
4. the winding fill factor is selected **60%** in the insulated region of the slot,
5. the main insulation is selected **0.5 mm**,

The outcome of the result shows that

1. the initial size D_o/D_i 270/160 is not enough to produce the desired torque,
2. the removal of tooth-tip would help to maximize current area and obtain more or less 15% more torque,
3. the SM²C core has to be supported with some higher permeability materials in order to facilitate field penetration through the core and also flux linkage with the windings.

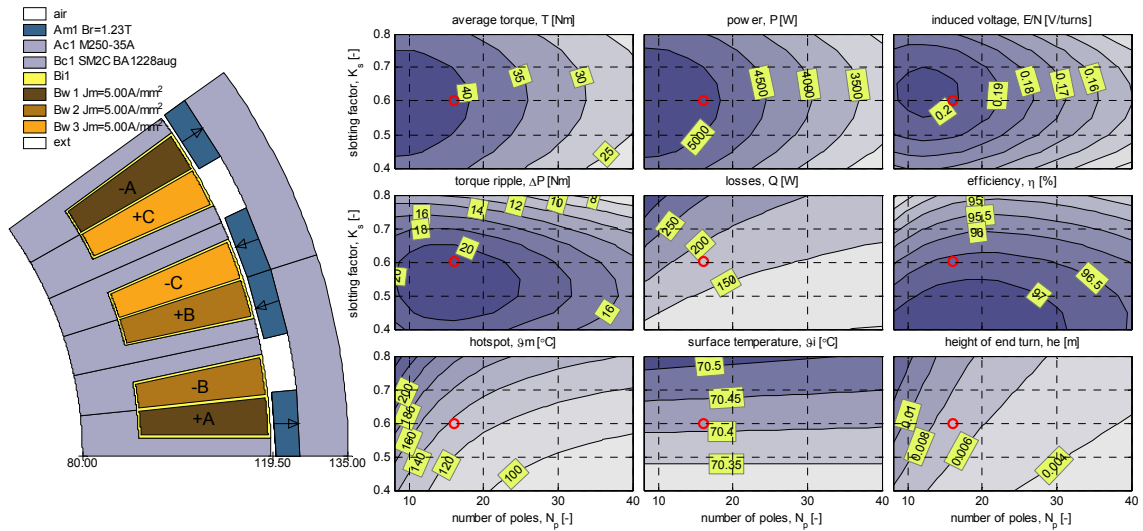


Figure 2.1 Machine layout at red dot on the maps and performance as a function of number of poles and the proportion between the winding and the core which is defined as slotting factor (more slot=more conductor)

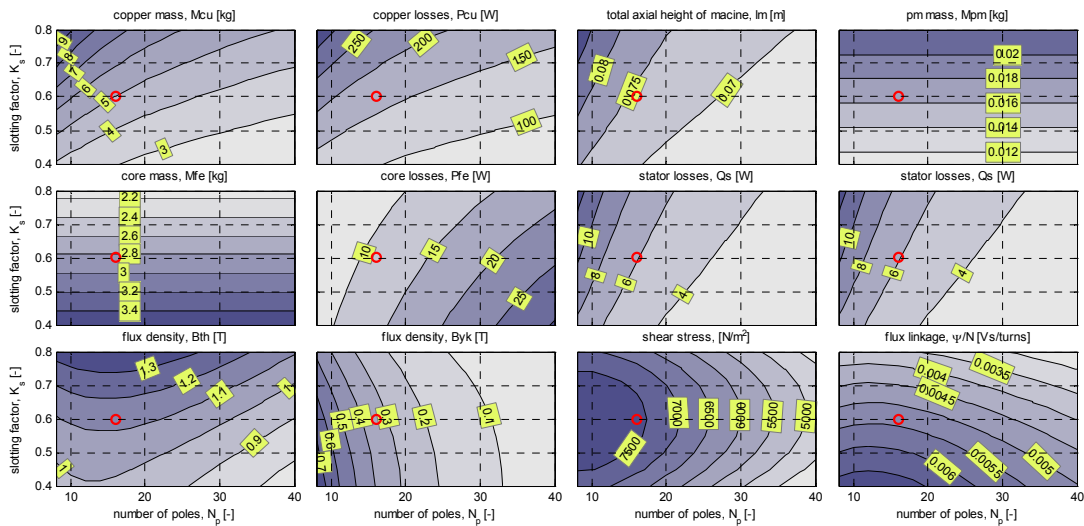


Figure 2.2 Continuation of machine design data as a function of number of poles and the proportion between the winding and the core which is defined as slotting factor (more slot=more conductor)

The previously defined machine size and layout (Figure 2.2) results a different amount of average torque and torque ripple (Figure 2.3).

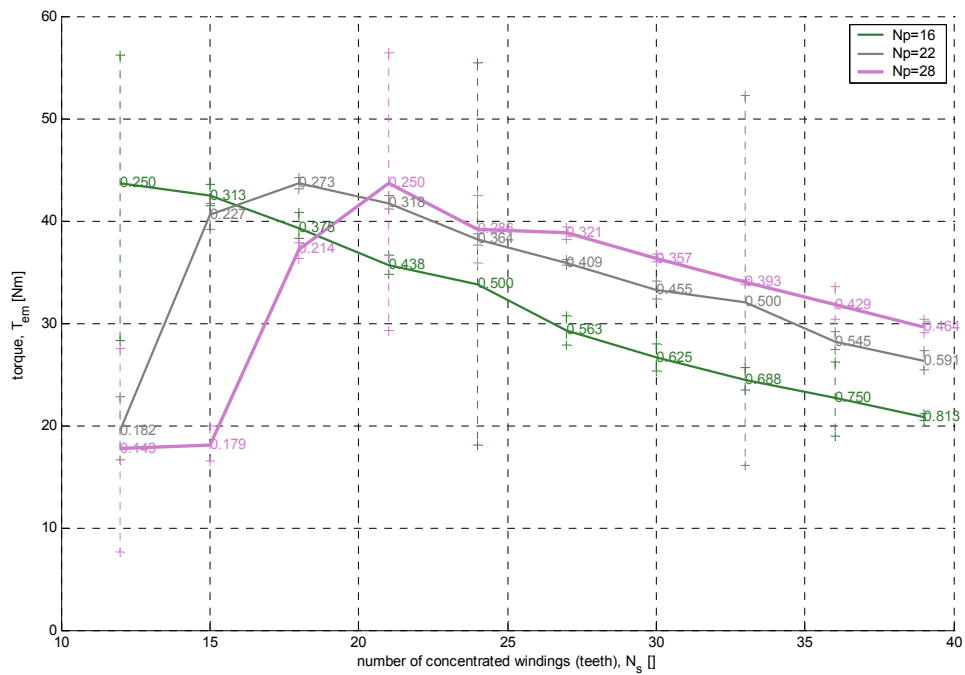


Figure 2.3 Average torque and torque ripple as a function of number of poles and number of slots or coils.

Figure 2.3 gives preference to 22P18S configuration even though this configuration does not result to a modular winding that might give a preference on wiring between the coils that belongs to the same phase.

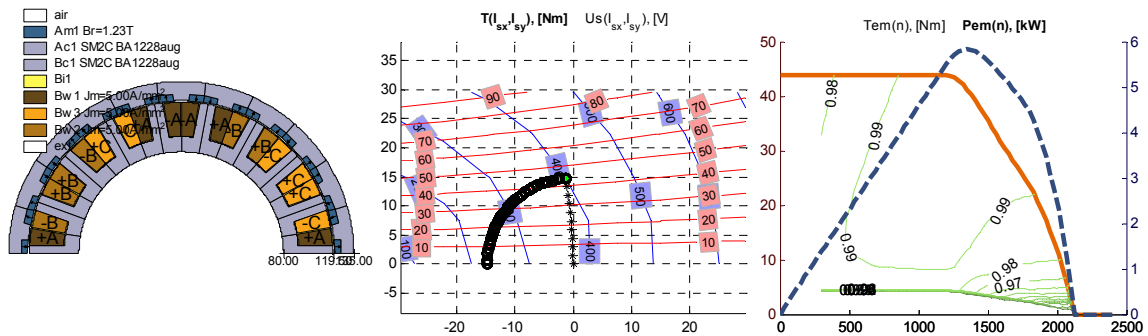


Figure 2.4 Machine layout (left), circle diagram (middle) and torque speed (right) of the proposed design.

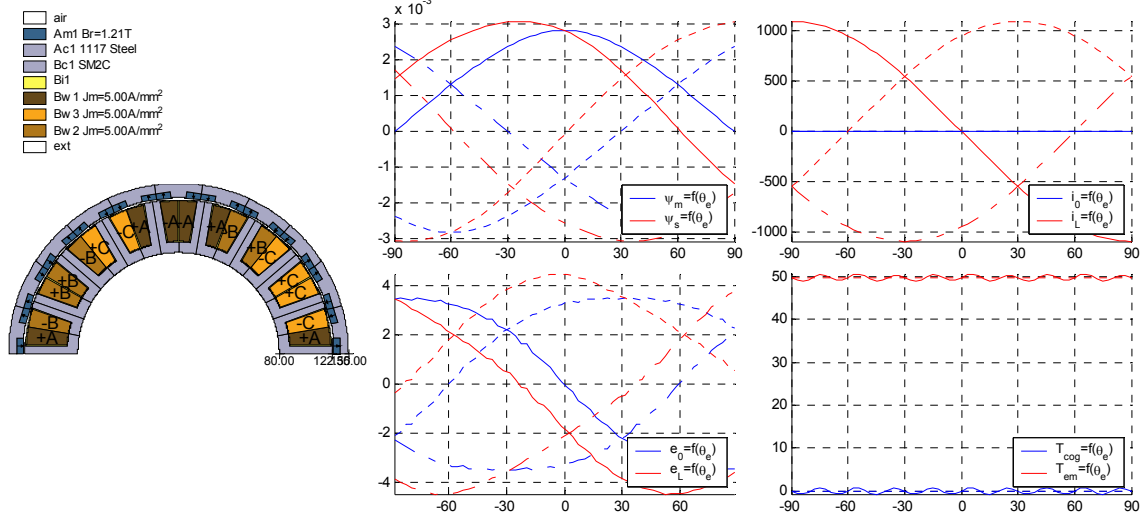


Figure 2.5 Selected machine characteristics: $K_m=0.7$, $R_g=123 \text{ mm}$,

As differences in Figure 2.4 and in Figure 2.5 reveal the design phase has reached to the point of working on details of design specification including the rotor specification where Figure 2.6 is given as an example. The main purpose of the design specification is to identify a simple manufacturable solution for the prototype.

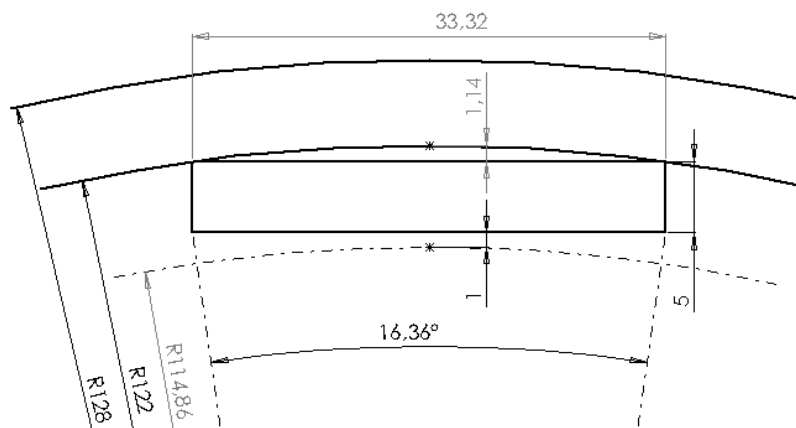


Figure 2.6 Details of rotor with surface mounted magnets

Different options for stator: 1) core material, 2) slot formation and 3) changes in proportions, and for rotor 4) permanent magnet size, and 5) mounting options have been studied a part of $N_p N_s$ selection shown in Figure 2.3.

2.2 Manufacturing experience of W1

The winding design has been updated from the initial height of 33.7 to 42.2 due to design updates ($\text{Ø}160/270 \rightarrow 120/256$) where more torque and simpler machine specification for manufacturing has been searched for.

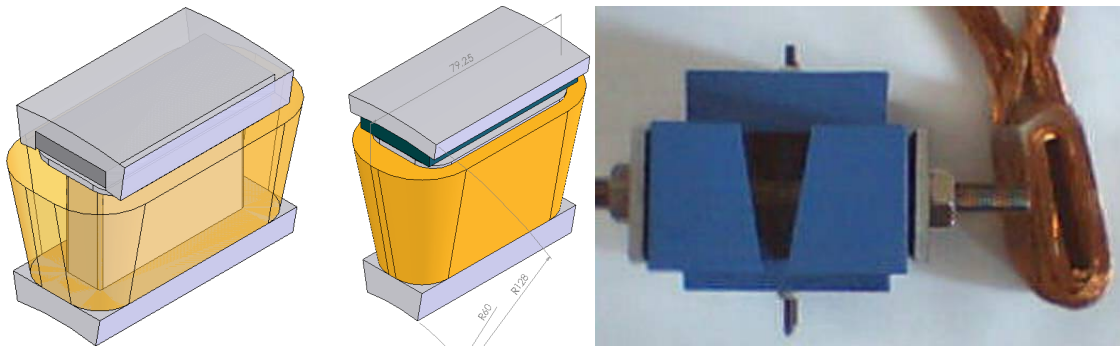


Figure 2.7 The initial design as a prototyping proposal (left), the final design developed because of the discussion of manufacturability and design target value (middle) and the manufactured test side (right).

For the series production of electric machine coils, a bobbin made of aluminum has been designed and manufactured, which enables the production of a phase coil consisting of two single coils and two paired coils.

3 Redesign of W1 resulting W2 and W3

In order to select the diameter of the hub and obtain the desired characteristics of the electric machine, the characteristics of the magnetic material with low magnetic permeability and low specific losses have been followed. This means that the length of the magnetization path must be as short as possible, and since the magnetization losses are expected to be low, the frequency can also be increased by increasing the pole pairs, which also shortens the length of the magnetization path as desired. Therefore, the thickness of the stator ring decreases, and the number of poles increases.

In the case of the new design, the focus is also on the availability and use of permanent magnets in mass production instead of choosing a permanent magnet with a special design and production sequence. Surface mounted permanent magnet (SPM) configuration is selected.

The design process starts from a fractional slot concentrated winding (FSCW) where number of slots per pole and phase is $q=0.5$ such as 24S16P, 21S14P but also $q=0.25$ such as 24S32P, 21S28P. Thereafter other pole/slot configurations are computed.

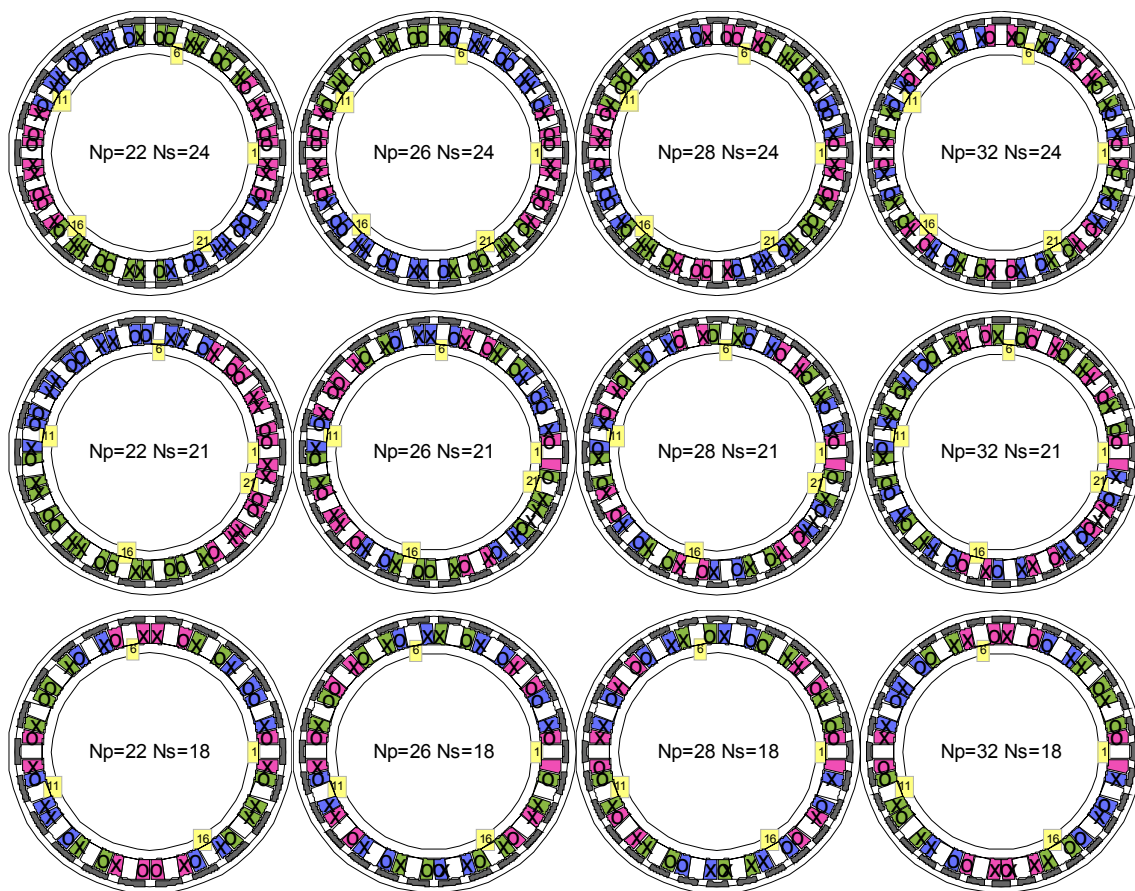


Figure 3.1 Winding layouts for a number of pole-to-slot configurations

3.1 Design of a medium $\varnothing 260$ and large $\varnothing 310$ PMSM

Figure 3.2 and Figure 3.3 show a number of design parameter variation over a design space where stator inner radius and number of poles are varied for $q=0.5$ FSCW SPM that reference size is $\varnothing 180/260$, respectively, Figure 3.4 and Figure 3.5 for machine that reference size is $\varnothing 240/310$.

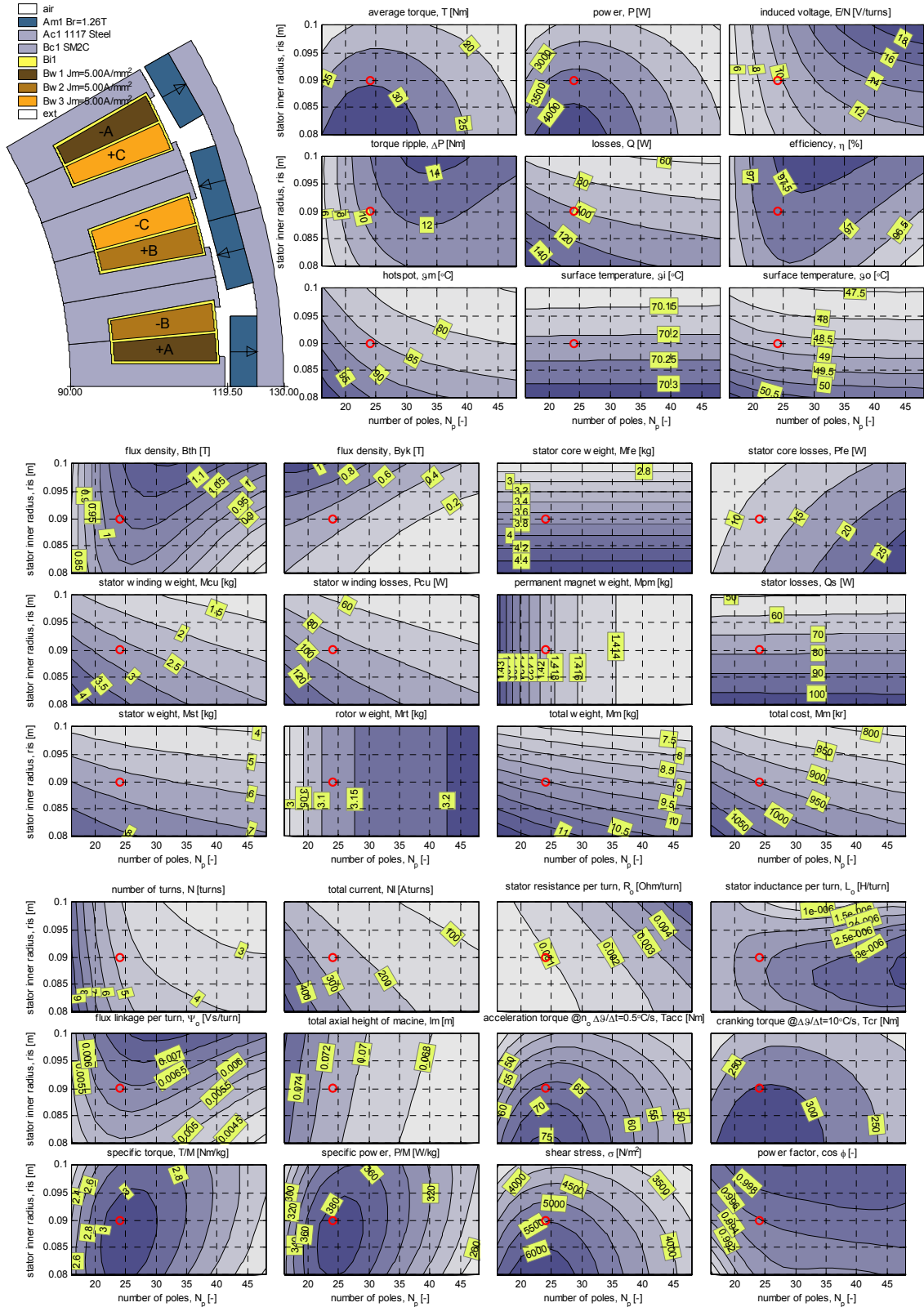


Figure 3.2 Design presentation FSCW SPM with $K_s = \text{slot width} / (\text{slot width} + \text{tooth width}) = 0.6$

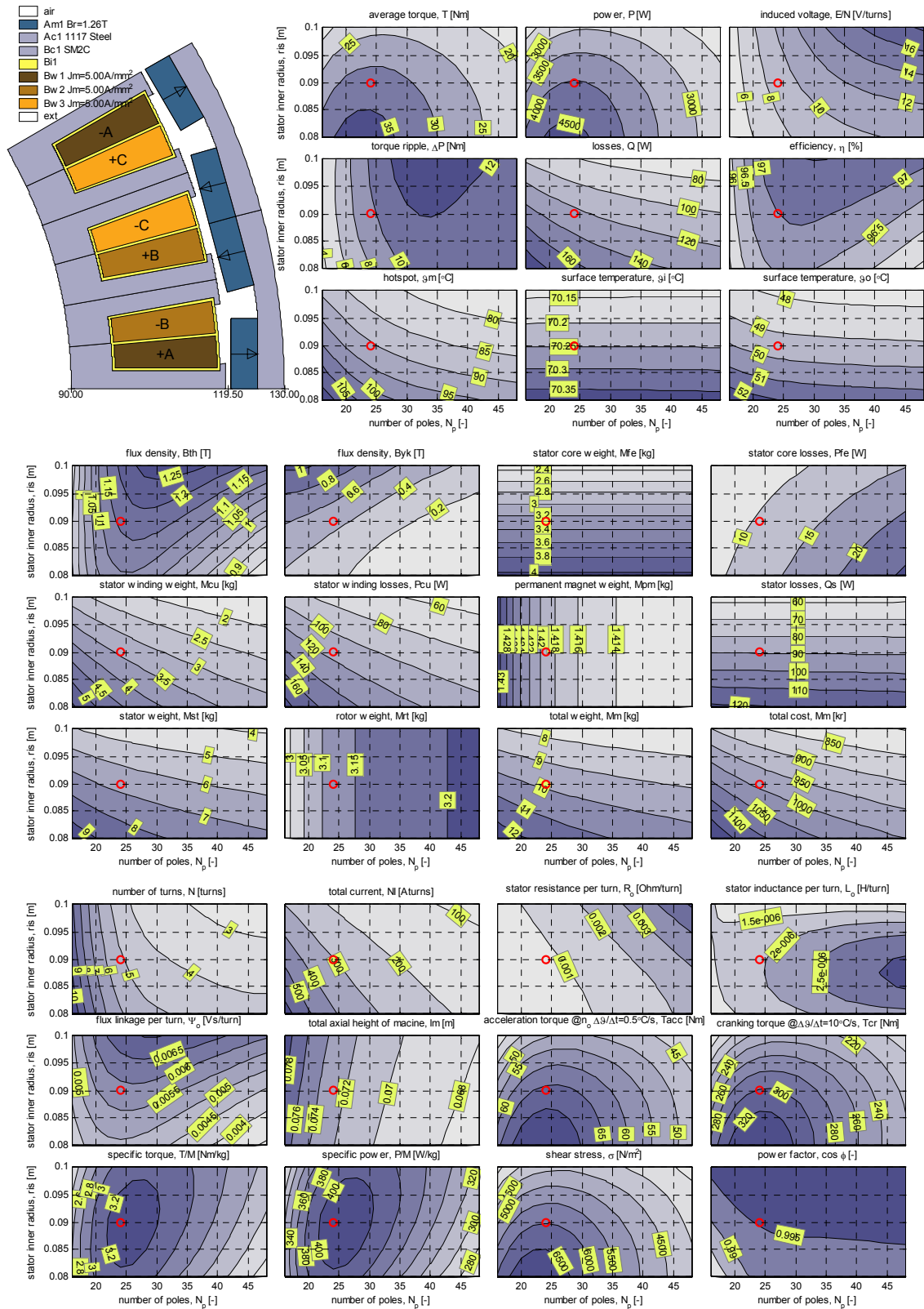


Figure 3.3 Design presentation FSCW SPM with $K_s = \text{slot width} / (\text{slot width} + \text{tooth width}) = 0.6$

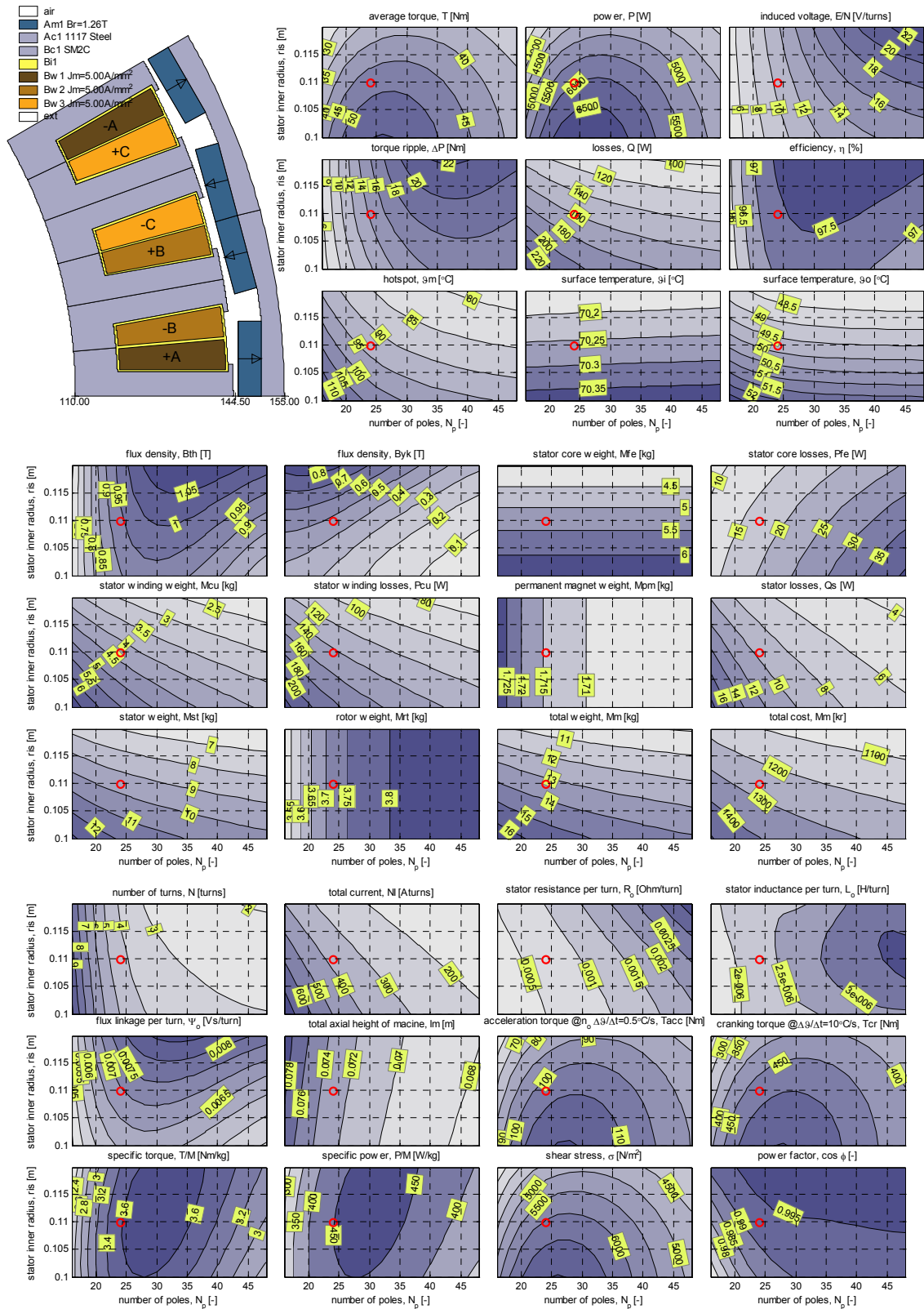


Figure 3.4 Design presentation FSCW SPM with $K_s = \text{slot width} / (\text{slot width} + \text{tooth width}) = 0.5$

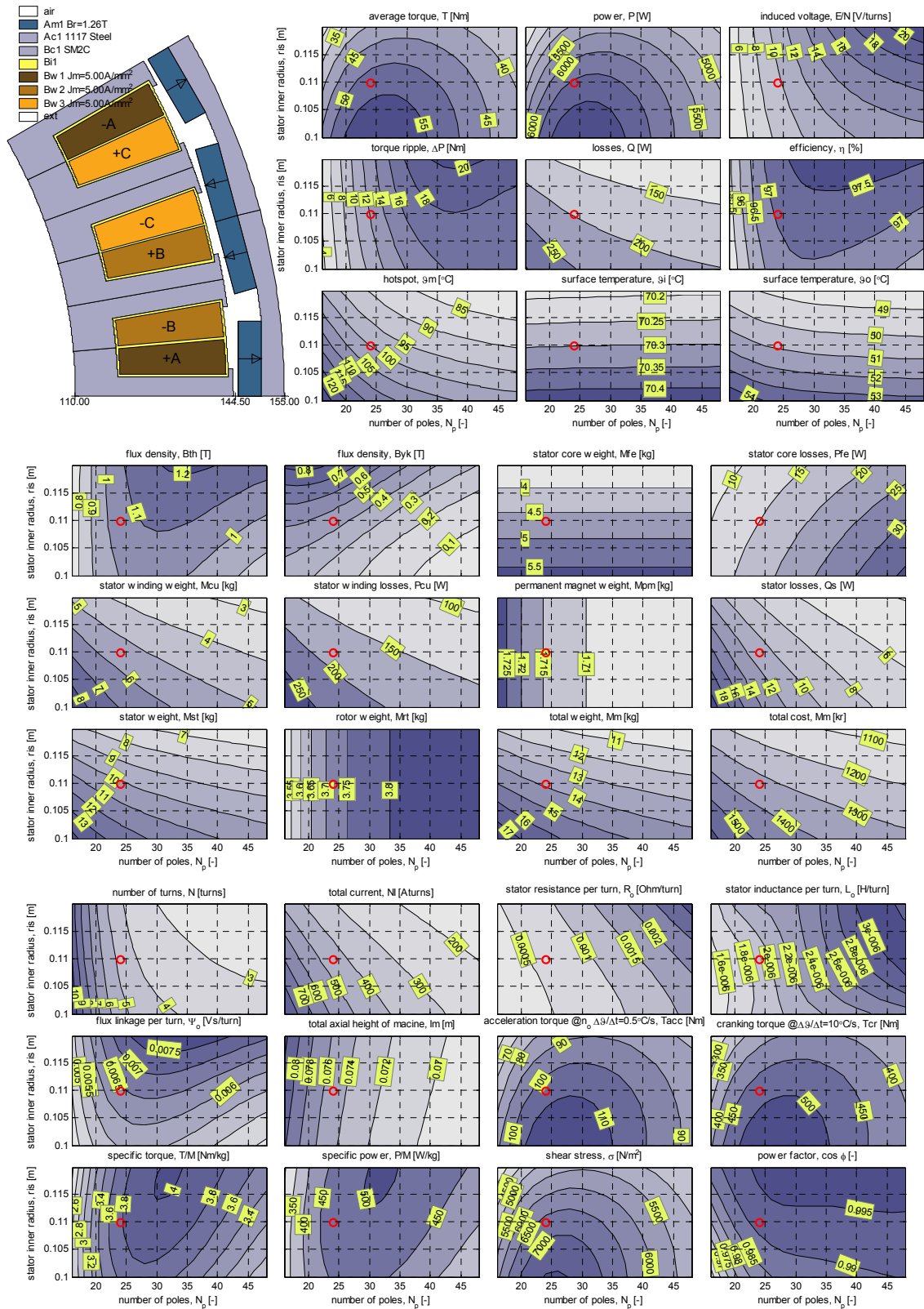


Figure 3.5 Design presentation FSCW SPM with $K_s = \text{slot width} / (\text{slot width} + \text{tooth width}) = 0.6$

3.2 Selection of pole-to-slot configuration

The pole-to-slot configuration is selected so that the expected torque mean value is high and torque ripple low. Torque quality/quantity curves for a specific configuration of a machine size: Ø180/260 and Ø240/310 are shown respectively in Figure 3.6 and Figure 3.7.

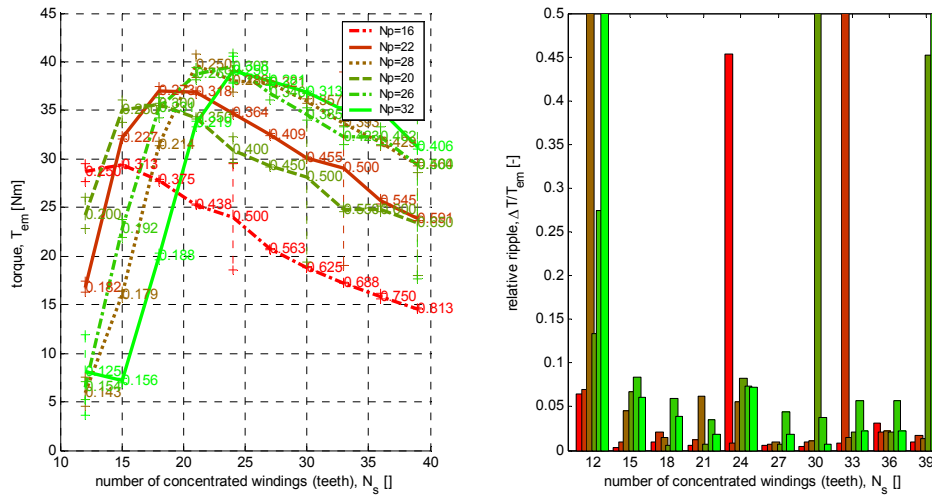


Figure 3.6 Torque and ripple as a function of number of poles- N_p and number of stator teeth- $N_t=N_s$ for Ø180/260 size of machine

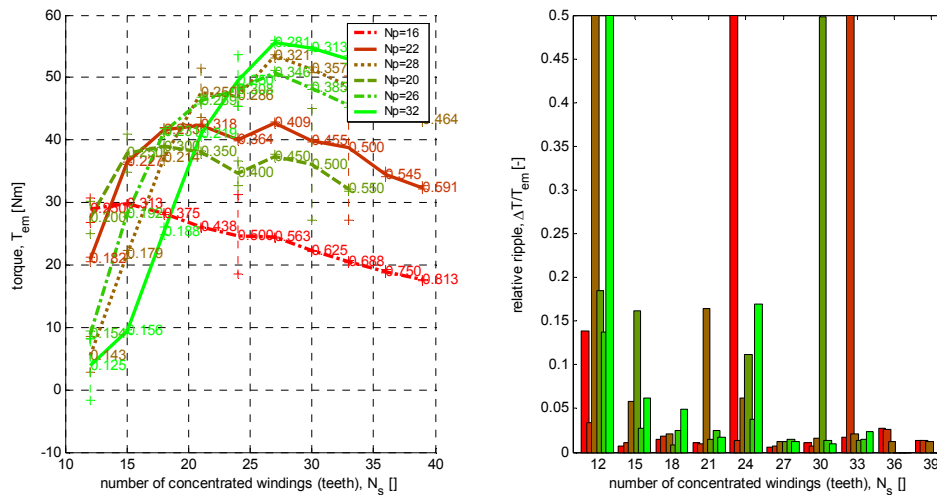


Figure 3.7 Torque and ripple as a function of number of poles- N_p and number of stator teeth- $N_t=N_s$ for Ø240/310 size of machine

Winding arrangement for the machines that establish the strongest magnetic coupling for this size of the machine is preferred especially when it provides a low torque ripple. The other criteria to be followed is if the pole-to-slot configuration provides pairs of modular coils like 22P24S, 28P30S or 26P24S and 32P30S so that $N_s=N_p \pm 2$ and N_s is multiple of 3. $N_s=N_p \pm 3$ is fine selection as it gives zero net force that is not the case with $N_s=N_p \pm 1$ (Figure 3.8). A next criterion is to keep number of poles and supply frequency preferably lower.

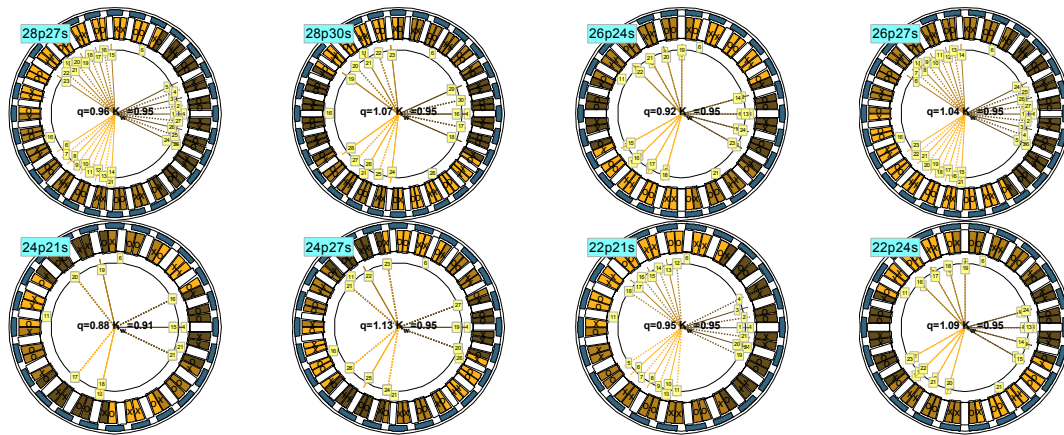


Figure 3.8 Visualization of modular winding where phase coils appear in groups and the spread of voltage vectors due to distribution of coils. The figure shows the numeric value for winding factor and q is shown here as ratio: N_s/N_p .

3.3 Comparison of baseline designs

Choosing a mass produced available NdFeB N36 60x8.5x5 block magnet the expected torque speed diagrams for designs W1 and W3 are shown in Figure 3.9. The importance here is not improvement in torque (compare Figure 2.4) rather than obtaining more rational design for prototyping.

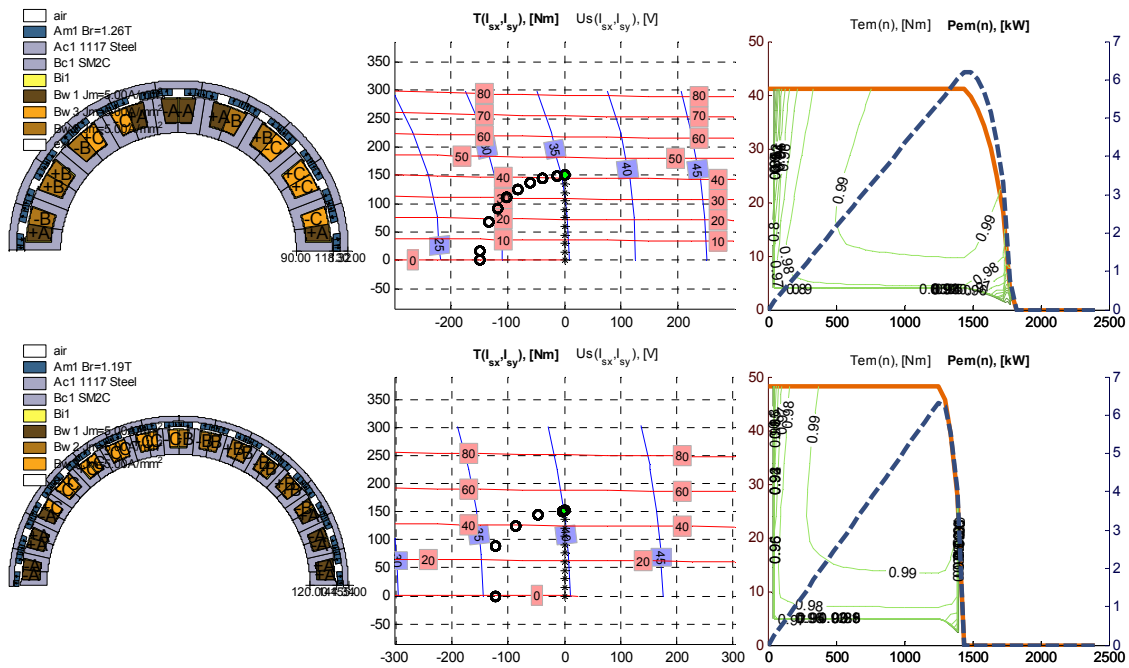
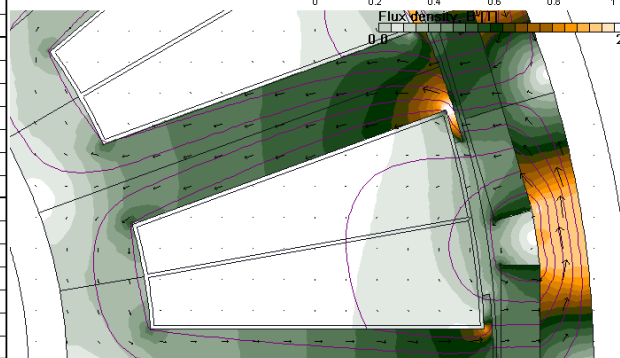
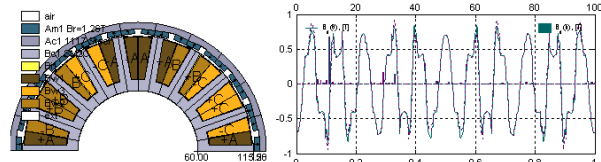


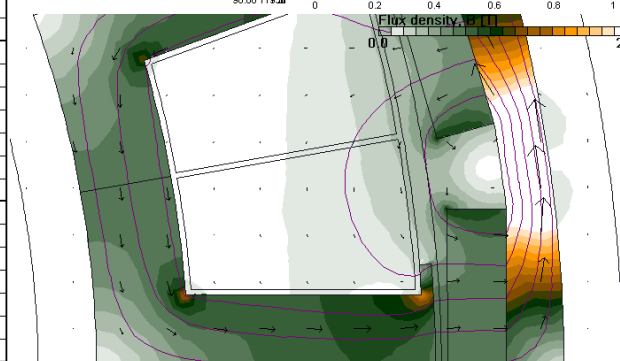
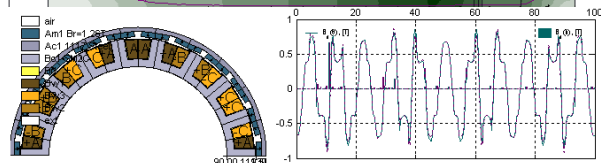
Figure 3.9 Machine, designs W2 up and W3 below, layout (left), circle diagram (middle) and torque speed (right) of the proposed design.

Figure 3.10 visualizes model-based comparison of baseline designs W1, W2 and W3.

quantity, unit	symbol=v		
radius, mm	ro=128.0	ri=60.0	rg=115.5
axial height, mm	hm=60.0	he=8.2	
radial length, mm	gap=1.0	hpm=5.0	
number, -	Np=22.0	Ns=18.0	
proportion, -	Kf=0.6	Ks=0.6	
weight, kg	Mc=7.9	Mf=4.4	Ms=12.3
weight, kg	Mm=1.3	Mf=2.4	Mr=3.7
current d., A/mm ²	Jc=5.0		
flux density, mT	Bg=672.5	Bt=637.1	By=324.2
flux linkage, mVs	Ψm=3.4	Ψs=3.6	
current, A	Ni=1246.3	Is=1526.5	
voltage, V	Em=4.6	Us=5.2	
torque, Nm	Te=56.3	Tn=56.3	
speed, krpm	no=1.2		
power, kW	Pi=7.3	Pe=7.1	Pn=7.1
power loss, W	Pc=266.8	Pf=7.0	Pm=10.0
efficiency, %	η=96.1		
cooling d., kW/m ²	Qc=12.1		
shear str., N/cm ²	MS=1.1		
sp. torque, Nm/kg	TM=3.5		
resistance, mΩ	Rs=0.1	Xs=1.2	



quantity, unit	symbol=v		
radius, mm	ro=130.0	ri=90.0	rg=119.5
axial height, mm	hm=60.0	he=11.6	
radial length, mm	gap=1.0	hpm=5.0	
number, -	Np=22.0	Ns=18.0	
proportion, -	Kf=0.6	Ks=0.6	
weight, kg	Mc=5.0	Mf=3.3	Ms=8.3
weight, kg	Mm=1.4	Mf=1.7	Mr=3.1
current d., A/mm ²	Jc=5.0		
flux density, mT	Bg=660.9	Bt=901.5	By=620.5
flux linkage, mVs	Ψm=4.6	Ψs=4.7	
current, A	Ni=647.3	Is=792.8	
voltage, V	Em=6.4	Us=6.7	
torque, Nm	Te=40.4	Tn=40.3	
speed, krpm	no=1.2		
power, kW	Pi=5.2	Pe=5.1	Pn=5.1
power loss, W	Pc=168.0	Pf=6.0	Pm=10.0
efficiency, %	η=96.5		
cooling d., kW/m ²	Qc=5.1		
shear str., N/cm ²	MS=0.7		
sp. torque, Nm/kg	TM=3.6		
resistance, mΩ	Rs=0.3	Xs=1.4	



quantity, unit	symbol=v		
radius, mm	ro=155.0	ri=120.0	rg=144.3
axial height, mm	hm=60.0	he=8.7	
radial length, mm	gap=1.0	hpm=5.0	
number, -	Np=28.0	Ns=30.0	
proportion, -	Kf=0.6	Ks=0.6	
weight, kg	Mc=3.7	Mf=3.7	Ms=7.4
weight, kg	Mm=1.6	Mf=2.3	Mr=3.8
current d., A/mm ²	Jc=5.0		
flux density, mT	Bg=691.2	Bt=946.0	By=724.3
flux linkage, mVs	Ψm=7.6	Ψs=7.7	
current, A	Ni=344.8	Is=422.3	
voltage, V	Em=13.4	Us=13.8	
torque, Nm	Te=45.2	Tn=45.1	
speed, krpm	no=1.2		
power, kW	Pi=5.8	Pe=5.7	Pn=5.7
power loss, W	Pc=126.4	Pf=9.5	Pm=10.0
efficiency, %	η=97.5		
cooling d., kW/m ²	Qc=3.0		
shear str., N/cm ²	MS=0.6		
sp. torque, Nm/kg	TM=4.0		
resistance, mΩ	Rs=0.7	Xs=3.7	

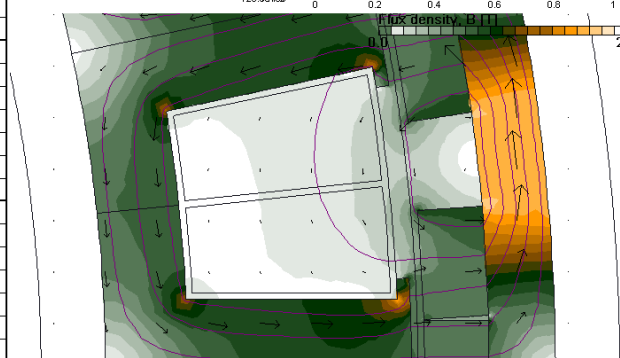
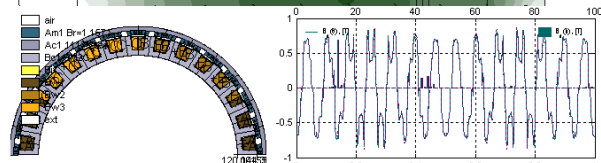


Figure 3.10 Model-based comparison of baseline designs W1 (top), W2 (middle) and W3 (bottom).

4 Prototyping and evaluation of a large Ø310 PMSM

The design evaluation comes with practical measures on how different parts should be manufactured and assembled:

1. winding segment production for moldable core process vs the process of winding if a hybrid core is used,
2. eventual connection and termination of stator coils and winding segments,
3. stator core “hybridization” when selecting and introducing different types of inserts,
4. If introducing additional parts for integration such as sensors, cooling channels then what is the impact to stator core and windings.

4.1 Short overview

The main outcome of machine production and performance evaluation is presented respectively in [7] and [6], while more general comparison of the design and material production is given in [1]. Based on 2D FE the expected Ø240/310 size machine performance when changing slot size and material properties is shown in Figure 4.1. More detailed image on the impact of core selection on magnetic loading of the stator core is visible in Figure 4.2.

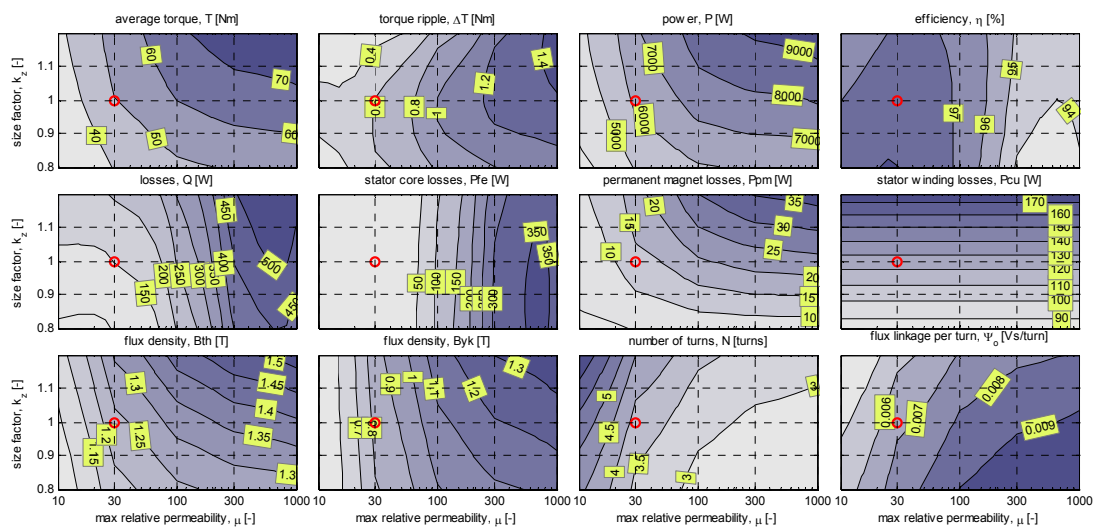


Figure 4.1 Maps of machine parameters as a function of maximum permeability of the core and the size of the slot (where slot tooth and yoke width is gradually changed).

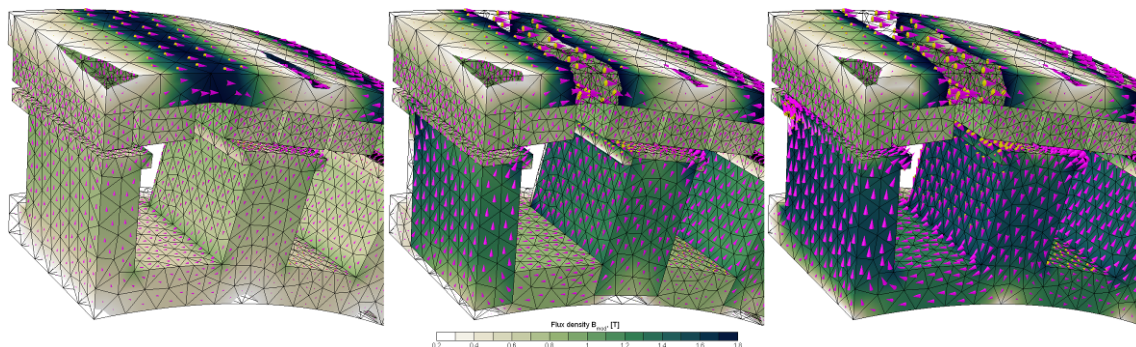


Figure 4.2 Flux linkage distribution for SM²C stator core (left), the same stator core with SMC inserts, and the core made of SMC.

If looking material selection and machine performance options in more generally (Figure 4.3) [1], then it is clear that the electrical machines with SM²C cores need to provide sufficiently inexpensive production that they remain to be attractive with their specific low torque capability compared to the other cores and solutions. It seems that SM²C machines can be more efficient at higher frequency and speed but still higher permeability couples more high frequency field that low permeability material is not able to attract (Figure 4.3). However, the high frequency leakage field

can easily produce power losses in the other structures and the whole solution is not as efficient anymore.

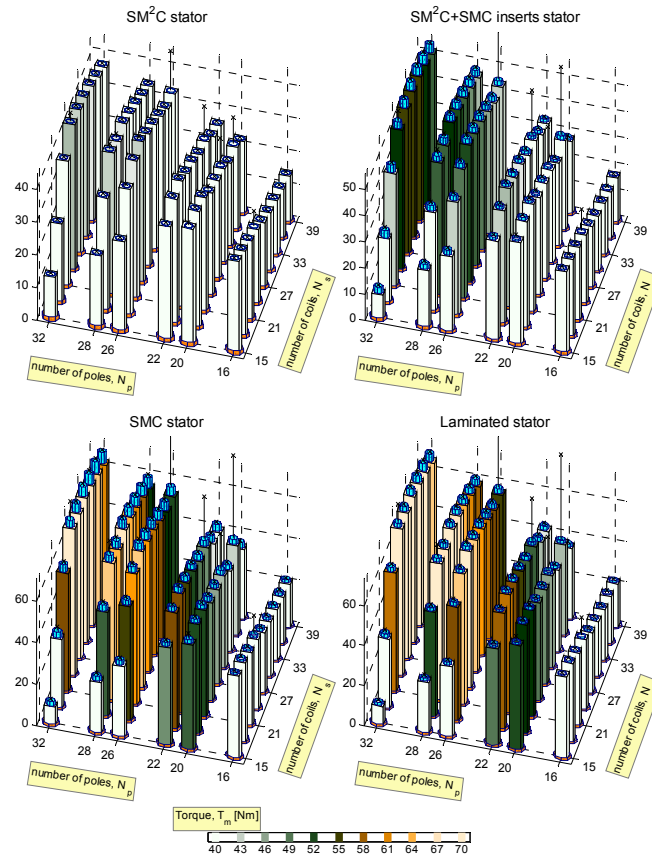


Figure 4.3 Average torque, ripple and losses as a drag torque over speed of four different stator of the Short & Wide machine.

The calculation (Figure 4.3), which is carried out in 2D FEA where the field-controlled machine is modeled, estimates the average torque, the torque ripple and the corresponding losses in the stator. The power losses in the windings are presented as a load torque at 900 rpm and the power losses in the core are at 9000 rpm [1]. The different speeds are selected to make the power losses more distinguishable as additional “internal load torque”. The following materials are included in this stage:

1. Soft magnetic moldable composite (SM²C) with maximum permeability of 16,
2. Compressed soft magnetic composite (SMC) in teeth regions and SM²C in the yoke,
3. Whole stator core made of SMC (Somaloy-P5) with maximum permeability more than 500,
4. Laminated stator (M250-35A) with maximum permeability more than 5000.

4.2 Manufactured stators and flux linkage comparison

Four complete stators are built (Table 4.1 and Figure 4.4) where for SMC Somaloy-3P is used. The stator core and coil data is provided in Table 4.2 and coil packing compared in Figure 4.5. Table 4.3 provides calculated values of magnetic flux linkage peak value per windings turn.

Table 4.1 Stator core specification

Short description of stator	Yoke	Teeth	Head
St1: Modular winding segments in SM ² C core	SM ² C	SM ² C	SM ² C
St2: Single tooth coils molded into SM ² C core	SM ² C	SMC	SM ² C
St3: Modular winding with SMC inserts	SM ² C	SMC	SM ² C
St4: Modular winding, inserts and wound yoke	Wire	SMC	SM ² C

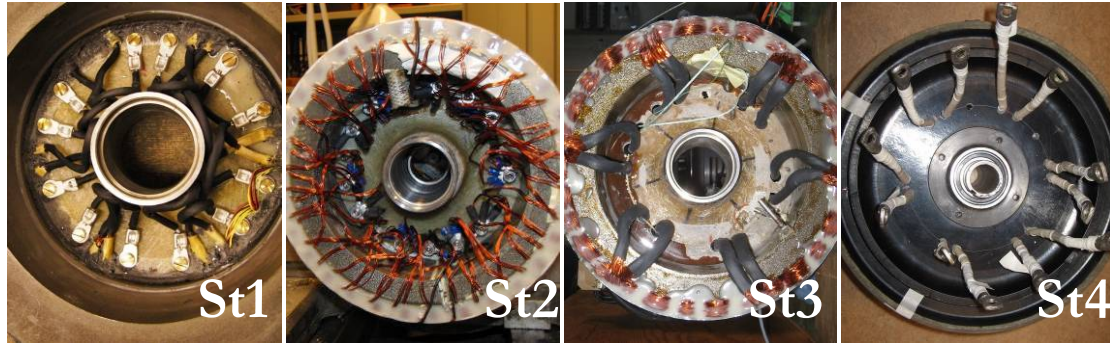


Figure 4.4 Stator prototypes

Table 4.2 Stator types and winding specification

Stator configuration	Strands & wire [mm]	Number of turns per tooth	Flux linkage [mVs]
St1: Modular winding segments in SM ² C core	17x0.8	12	2.16
St2: Single tooth coils molded into SM ² C core	3x1.0	5x30	3.73
St3: Modular winding with SMC inserts	70x0.65	3	3.48
St4: Modular winding, inserts and wound yoke	70x0.65	3	3.87

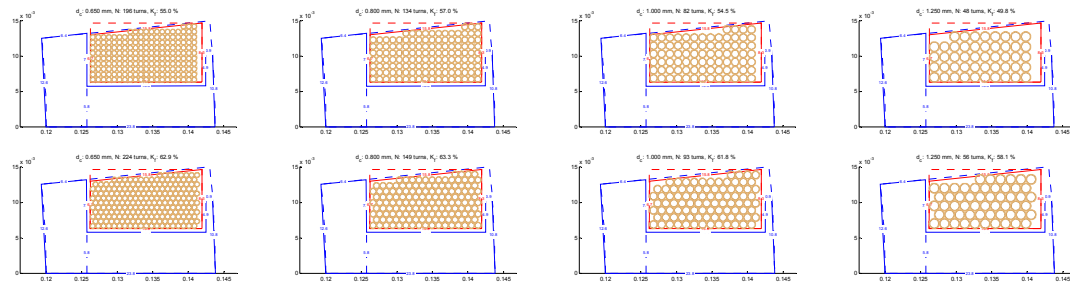


Figure 4.5 coil cross-section and coil packing visualization

By citing conclusion in [6] the following is stated about the magnetic performance of the cores based to magnetic flux linkage evaluations: Based on the calculation and experimental estimation of flux linkage it can be stated that the results comparing quite well. Still the discrepancy becomes bigger with SM²C core alone, which can indicate that the molding process can cause larger difference in geometry and material properties inside the molded core. However, inserts improve the design with the cost of reduction on energy conversion efficiency. The wound insert (St4) has relatively low flux linkage, which is likely due to additional reluctance between the ferrous (yoke) core and SMC insert.

From a construction point of view the SM²C core is attractive for high frequency applications that give single step assembling with high integrity. As a matter of fact, the low permeability causes low torque capability, which in turn depends on geometric complexity and fill rate (further visualized in Figure 4.6). The high permeability inserts increase the torque capability with multi-step production.

Table 4.3 FE-based flux linkage values

Stator core description and	2D FE	3D FE
Whole core SM ² C no inserts	2.61	2.66
Short Somaloy-3P @ 1.1GP inserts	3.47	-
Long Somaloy-3P @ 1.1GP inserts	3.71	3.49
Core Somaloy-3P @ 1.1GP inserts	4.42	-
Yoke Somaloy-3P @ 1.1GP inserts	3.04	-
Whole core Somaloy-3P @ 1.1GP	4.58	4.57
Short Somaloy-5P @ 0.8GP inserts	3.48	-
Long Somaloy-5P @ 0.8GP inserts	3.67	3.45
Core Somaloy-5P @ 0.8GP inserts	4.40	-
Yoke Somaloy-5P @ 0.8GP inserts	3.03	-
Whole core Somaloy-5P @ 0.8GP	4.55	4.53

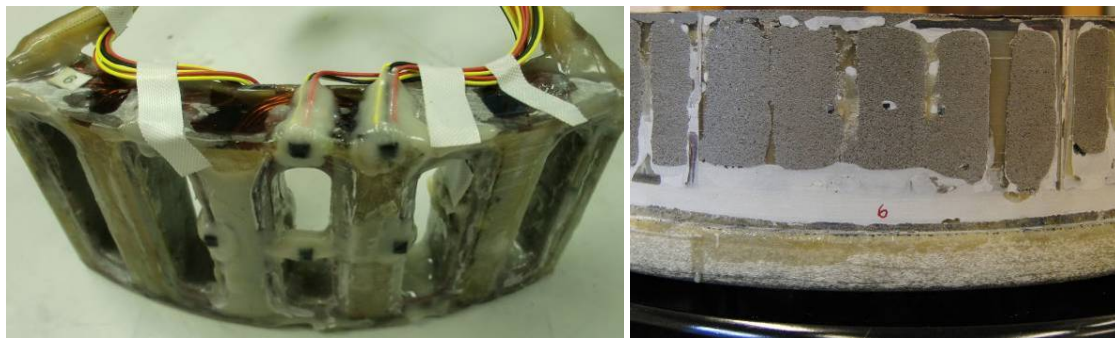


Figure 4.6 Inclusion of ball sensors (left) and their location after molding and machining (right)

Details related to hub motor vector control and also position feedback are described in [3].

4.3 Evaluation process

The SM²C stator (ST1) and the stator with teeth-inserts (ST2) measurement results are presented in this section. The scope of the measurements is to investigate the magnetic coupling, torque capability and torque quality in terms of cogging and torque ripple.

Short summary:

- Stator core with inserts (ST2) has 1.7 times higher flux linkage as SM²C stator (ST1),
- Reduction of flux linkage by increased speed has likely to do with the rotor power loss (including B_r reduction by temperature) but it is unproved, machine has to reach first to nominal speed and slightly beyond that mechanically,
- When using distributed concentrated coils as the winding, the coils need to be connected in series to avoid circulating currents. ST2 stator is well suited to lower speed or higher voltage application due to higher number of turns.

The back emf measurements of the selected machines (ST1 ST2 that are presented here) is performed in the mounting bench (Figure 4.7).

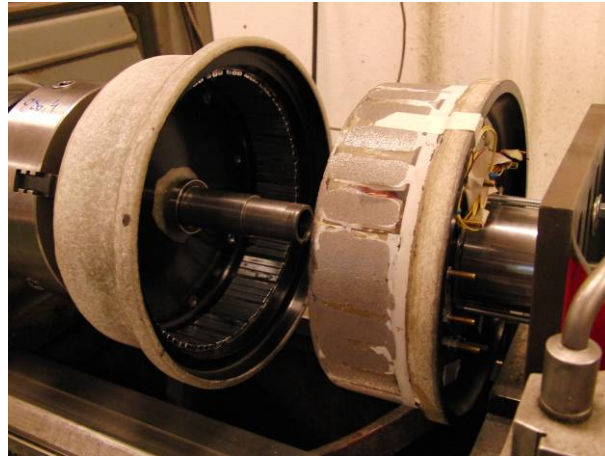


Figure 4.7 Machine mounting and test bench

Alternatively, the test machine is driven with a power tool to provide speed, measure induced voltage and integrate magnetizing flux linkage (Figure 4.8). With stator ST1 the back emf development is observed in the range of 21 to 84 Hz (90 to 360 rpm), which shows that the back emf is not increasing linearly (Table 4.4 and Figure 4.13 left also repeated Table 4.8 and Figure 4.13 right). Therefore, several investigations have started to find out the reasons of dynamic damping of magnetizing flux with the increasing speed. There are no signs that any damping phenomena lies in the stator according to RLC measurements of stator only (Table 4.5). Consequently, the measurements of induced voltages from the pick-up coil around the single surface mounted magnets are initiated (Table 4.6). As the thickness of the rotor yoke is minimized and becomes saturated at the alignment it is expected that the variation of rotor reluctance exaggerates the dynamic damping phenomenon in the rotor (apart from harmonic content caused by the usage of distributed concentrated winding). A test coil of 5 turns is wound around the magnets. The measurement confirms (Figure 4.9) that the flux variation of the magnets is double of the magnetization frequency, but the experimentation does not explicate the loss mechanisms in the rotor. At this moment, the machine is tested with the drive system designed for that. The analogous hall (integrated) sensor (Figure 4.6 at end turn region) does not form a perfect resolver feedback as the sensors goes to saturation. The digital sensors (Figure 4.6 3 in a row in the middle) function perfect including the position observer. Unfortunately, no additional experimentation has been made in motor operation due to lack of test bench and mechanical unbalance that increases risk to run machine faster than 600 rpm. Cogging and ripple torque of ST1 is larger than expected; the torque capability is 2/3 as it is expected. Since the rotor geometry is “adapted” to the new (ST2) stator, the back emf measurements are repeated for the existing (ST1) (Figure 4.11 and Table 4.8) but they are carried out at parallel (Figure 4.10 and Table 4.7) and per coil measurement (Figure 4.12 and Table 4.9) for the (ST2) stator. In fact, there are neither measurements of cogging torque nor experiments on motor operation due to high friction torque.

Measurements in chronological order:

1. Back emf measurement and flux linkage estimation of ST1,
2. RLC measurement of ST1,
3. Induced voltage measurements across pick-up coils around the magnets,
4. emf measurement and flux linkage estimation of ST2,
5. Repeated emf measurement and flux linkage estimation of ST1.

EMF Measurement of 5-serie coupled 12 turn winding segments

Induced voltage divided by magnetization speed ($n/60 \cdot 2\pi \cdot 2/N_p$) and the number of turns $N_t=12$, and the integration of the back emf at the highest test speed $n=360$ rpm.

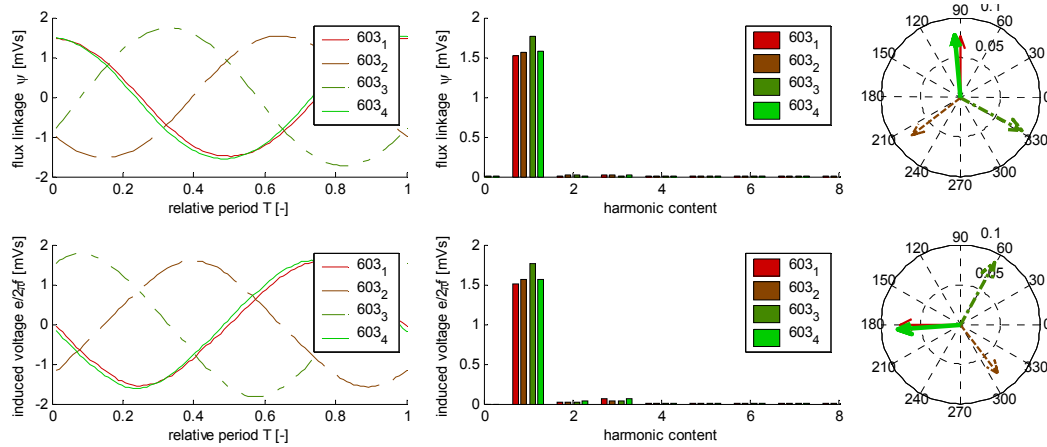


Figure 4.8 Voltage and flux linkage waveforms and phasors (ST1)

Table 4.4 Test results at selected speed and selected phase sections

Test winding	Ψ_{m1} , [mVs]	Ψ_{rms} , [mVs]	Ψ_{THD} , [%]	E_{m1} , [mV]	E_{rms} , [mV]	E_{THD} , [%]	Freq, [Hz]	Shift, [deg]
Ph-a Sc-1	2.16	1.51	0.0	2.14	1.50	0.0	21.4	0
Ph-b Sc-1	2.17	1.52	0.0	2.17	1.52	0.0	21.4	125.8
Ph-c Sc-1	2.44	1.71	0.0	2.45	1.72	0.0	21.4	241.5
Ph-a Sc-2	2.18	1.52	0.0	2.15	1.50	0.1	21.4	2.5
Ph-a Sc-1	2.09	1.46	0.0	2.07	1.45	0.0	37.3	0
Ph-b Sc-1	2.05	1.43	0.0	2.05	1.43	0.0	37.3	125.9
Ph-c Sc-1	2.37	1.66	0.0	2.38	1.67	0.0	37.3	-121.4
Ph-a Sc-2	2.23	1.56	0.0	2.21	1.55	0.1	37.3	-3.6
Ph-a Sc-1	2.15	1.51	0.0	2.13	1.49	0.0	84.0	0
Ph-b Sc-1	2.19	1.53	0.0	2.21	1.55	0.0	84.0	127.1
Ph-c Sc-1	2.51	1.75	0.0	2.51	1.76	0.0	84.0	-120.0
Ph-a Sc-2	2.23	1.56	0.0	2.21	1.55	0.1	84.0	-2.6
Ph-a Sc-1	2.11	1.48	0.0	2.09	1.46	0.0	65.1	0
Ph-b Sc-1	2.05	1.44	0.0	2.05	1.44	0.0	65.1	127.6
Ph-c Sc-1	2.38	1.67	0.0	2.40	1.68	0.0	65.1	118.8
Ph-a Sc-2	2.26	1.58	0.0	2.23	1.56	0.1	65.1	5.1
Ph-a Sc-1	2.09	1.46	0.0	2.06	1.45	0.0	70.1	0
Ph-b Sc-1	2.22	1.56	0.0	2.23	1.56	0.0	70.1	120.6
Ph-b Sc-2	2.19	1.53	0.0	2.20	1.54	0.0	70.1	119.4
Ph-c Sc-2	2.22	1.55	0.0	2.24	1.57	0.1	70.1	-121.2
Ph-a Sc-1	2.16	1.51	0.0	2.13	1.50	0.0	37.3	0
Ph-b Sc-1	2.14	1.50	0.0	2.15	1.51	0.0	37.3	125.6
Ph-b Sc-2	2.26	1.58	0.0	2.25	1.58	0.0	37.3	115.0
Ph-c Sc-2	2.39	1.67	0.0	2.42	1.69	0.1	37.3	-123.4

When comparing the averaged flux linkage value over the table to the expected value from the calculations then the test machine shows about 10-11% lower value. (Author's note: The earlier 1/3 difference is "reduced" by implementing more accurate data about material properties.)

RLC Measurement of 5-serie coupled 12 turn winding segments

RLC measurements (Table 4.5) are taken by using HAMEG.

Table 4.5 Measurement of resistance, inductance, and capacitance of phase segments and between the phase segments

Phase segment	Quantity and unit	100 Hz	120 Hz	1 kHz	10 kHz	25 kHz
1 Ph-a Sc-1	R, [Ohm]	0.029	0.030	0.030	0.132	0.583
	L, [μ H]	103	103	103.2	102.0	100.6
	C, [mC]	24.3	16.9	0.245	2.48e-3	403e-6
2 Ph-b Sc-1	R, [Ohm]	0.030	0.030	0.038	0.166	0.616
	L, [μ H]	112	111	110.6	107.2	105.7
	C, [mC]	22.8	15.6	0.229	2.36e-3	383e-6
4 Ph-c Sc-1	R, [Ohm]	0.036	0.036	0.036	0.176	0.844
	L, [μ H]	140	139	139.0	137.6	135.6
	C, [mC]	18.1	12.6	0.182	1.84e-3	298e-6
5 Ph-a Sc-2	R, [Ohm]	0.031	0.031	0.033	0.139	0.748
	L, [μ H]	116	116	115.6	113.4	111.4
	C, [mC]	22.9	15.1	0.219	2.23e-3	644e-6
6 Ph-b Sc-2	R, [Ohm]	0.032	0.032	0.033	0.174	0.714
	L, [μ H]	120	119	119.8	118.0	116.2
	C, [mC]	21.1	14.6	0.211	2.14e-3	348e-6
7 Ph-c Sc-2	R, [Ohm]	0.032	0.031	0.033	0.180	0.769
	L, [μ H]	117	116	116.8	115.0	113.1
	C, [mC]	21.6	14.9	0.216	2.203e-3	358e-6
1-7	R, [MOhm]	66	44	1.42	0.2236	0.149
	L, [μ H]					
	C, [pC]	398	394	313	119	91
1-4	R, [Ohm]	43	30	1.07	0.290	
	L, [μ H]					
	C, [pC]	404	408	260	75.8	59

EMF measurement of pick-up-coils placed around the magnets

5 turn pick up coils are placed around three magnets: two from the opposing sides and one from the middle. The flux linkage and emf per speed values are taken 20 times bigger in the graph and table for the sake of visibility.

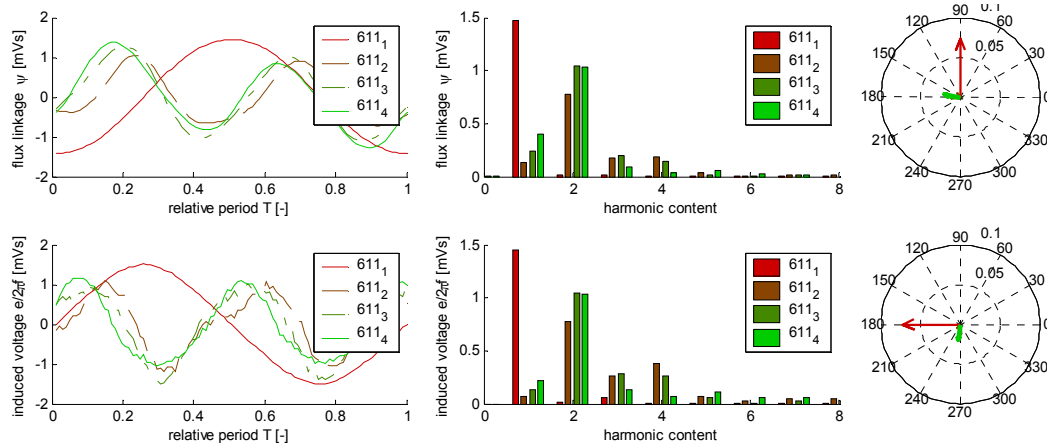


Figure 4.9 Induced voltage and integrated flux linkage waveforms from pick-up coils

Table 4.6 Test results at selected speed and selected coils

Test winding	Ψ_{m1} , [mVs]	Ψ_{rms} , [mVs]	Ψ_{THD} , [%]	E_{m1} , [mV]	E_{rms} , [mV]	E_{THD} , [%]	Freq, [Hz]	Shift, [deg]
Ph-a Sc-1	2.08	1.45	0.0	2.06	1.44	0.0	22.5	0
Magnet 1	0.78	0.55		0.77	0.54		22.5	
Magnet 2	1.04	0.73		1.05	0.74		22.5	
Magnet 3	1.03	0.72		1.03	0.72		22.5	
Ph-a Sc-1	2.06	1.44	0.0	2.04	1.43	0.0	28.0	0
Magnet 1	0.97	0.68		0.95	0.67		28.0	
Magnet 2	0.87	0.61		0.86	0.60		28.0	
Magnet 3	0.94	0.66		0.96	0.67		28.0	
Ph-a Sc-1	2.13	1.49	0.0	2.11	1.48	0.0	39.3	0
Magnet 1	0.92	0.65		0.92	0.65		39.3	
Magnet 2	0.75	0.53		0.76	0.53		39.3	
Magnet 3	1.07	0.75		1.04	0.73		39.3	
Ph-a Sc-1	2.00	1.40	0.0	1.98	1.38	0.0	46.3	0
Magnet 1	0.81	0.57		0.82	0.57		46.3	
Magnet 2	1.03	0.72		1.02	0.72		46.3	
Magnet 3	0.96	0.67		0.96	0.67		46.3	

The permanent magnet flux variation due to reluctance change is detected and estimated but the deeper analysis of loss mechanism, influence on flux linkage reduction by increase of rotation speed is not carried further based on this data, and a thermal measurement is carried out to investigate the induced rotor losses.

Measurement of 5-parallel coupled 30-turn coils

Induced voltage divided by magnetization speed ($n/60 \cdot 2\pi \cdot 2/N_p$) and the number of turns $N_t=30$, and the integration of the back emf at the highest test speed $n=50$ rpm.

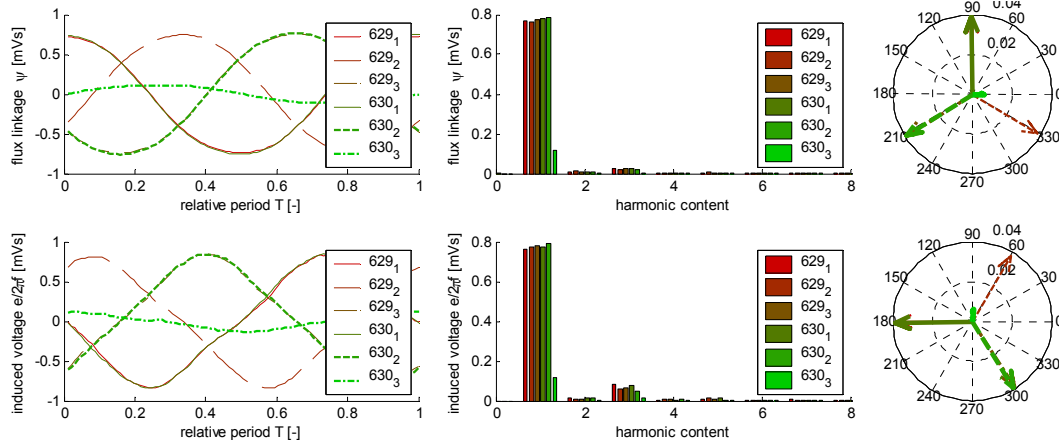


Figure 4.10 Voltage and flux linkage waveforms and phasors (ST2)

Table 4.7 Test results at selected speed and selected phase sections (ST2)

Test winding	Ψ_{m1} , [mVs]	Ψ_{rms} , [mVs]	Ψ_{THD} , [%]	E_{m1} , [mV]	E_{rms} , [mV]	E_{THD} , [%]	Freq, [Hz]	Shift, [deg]
Ph-a Sc-1	0.73	0.51	0.0	0.72	0.51	0.0	4.8	0
Ph-b Sc-1	0.72	0.50	0.0	0.72	0.51	0.0	4.8	-119.5
Ph-c Sc-1	0.71	0.50	0.1	0.71	0.50	0.6	4.8	119.4
Ph-a Sc-2	0.79	0.55	0.0	0.78	0.55	0.0	4.8	0.56
Ph-b Sc-2	0.75	0.53	0.0	0.76	0.53	0.0	4.8	121.8
Ph-c Sc-2	0.12	0.09	0.1	0.12	0.09	0.6	4.8	-103.2
Ph-a Sc-1	0.74	0.52	0.0	0.73	0.52	0.0	6.0	0
Ph-b Sc-1	0.73	0.51	0.0	0.73	0.51	0.0	6.0	-119.5
Ph-c Sc-1	0.74	0.52	0.1	0.74	0.52	0.6	6.0	119.3
Ph-a Sc-2	0.78	0.55	0.0	0.77	0.54	0.0	6.0	1.1
Ph-b Sc-2	0.80	0.56	0.0	0.81	0.57	0.0	6.0	118.0
Ph-c Sc-2	0.12	0.08	0.1	0.12	0.09	0.6	6.0	-98.5
Ph-a Sc-1	0.75	0.53	0.0	0.74	0.52	0.0	7.6	0
Ph-b Sc-1	0.76	0.53	0.0	0.76	0.53	0.0	7.6	-119.0
Ph-c Sc-1	0.76	0.53	0.1	0.76	0.53	0.6	7.6	121.0
Ph-a Sc-2	0.77	0.54	0.0	0.76	0.54	0.0	7.6	-0.84
Ph-b Sc-2	0.77	0.54	0.0	0.77	0.54	0.0	7.6	117.9
Ph-c Sc-2	0.12	0.09	0.1	0.12	0.09	0.6	7.6	-105.2
Ph-a Sc-1	0.76	0.53	0.0	0.75	0.53	0.0	9.6	0
Ph-b Sc-1	0.77	0.54	0.0	0.77	0.54	0.0	9.6	-117.5
Ph-c Sc-1	0.74	0.52	0.1	0.75	0.53	0.6	9.6	120.6
Ph-a Sc-2	0.78	0.55	0.0	0.78	0.55	0.0	9.6	0.11
Ph-b Sc-2	0.75	0.53	0.0	0.76	0.53	0.0	9.6	118.3
Ph-c Sc-2	0.12	0.08	0.1	0.12	0.08	0.6	9.6	-103.4
Ph-a Sc-1	0.77	0.54	0.0	0.76	0.54	0.0	12.1	0
Ph-b Sc-1	0.76	0.54	0.0	0.77	0.54	0.0	12.1	-121.0
Ph-c Sc-1	0.77	0.54	0.1	0.78	0.55	0.6	12.1	122.6
Ph-a Sc-2	0.78	0.55	0.0	0.78	0.55	0.0	12.1	0.88
Ph-b Sc-2	0.78	0.55	0.0	0.79	0.55	0.0	12.1	122.1
Ph-c Sc-2	0.12	0.08	0.1	0.11	0.08	0.6	12.1	-94.6

Measurement of 5-serie coupled 12 turn winding segments

Induced voltage divided by magnetization speed ($n/60 \cdot 2\pi \cdot 2/N_p$) and the number of turns $N_t=12$, and the integration of the back emf at the highest test speed $n=400$ rpm.

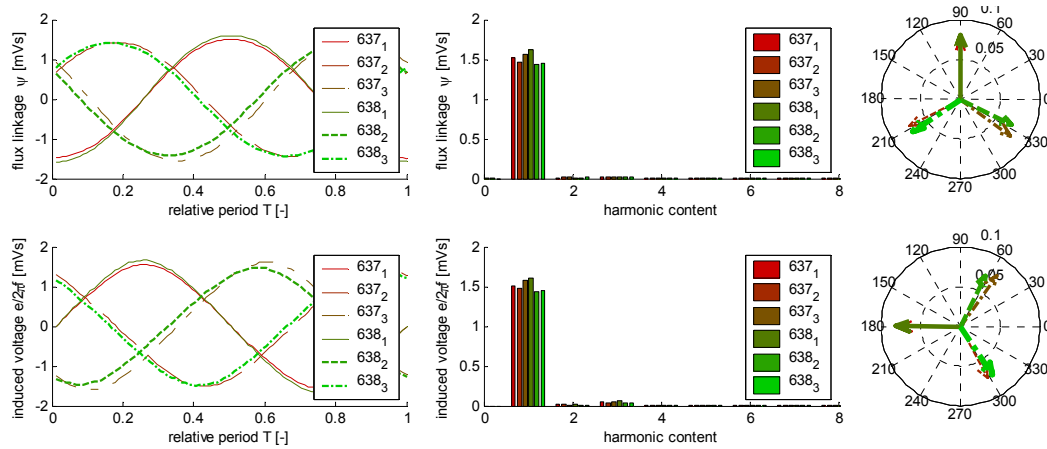


Figure 4.11 Voltage and flux linkage waveforms and phasors (ST1)

Table 4.8 Test results at selected speed and selected phase sections (ST1)

Test winding	Ψ_{m1} , [mVs]	Ψ_{rms} , [mVs]	Ψ_{THD} , [%]	E_{m1} , [mV]	E_{rms} , [mV]	E_{THD} , [%]	Freq, [Hz]	Shift, [deg]
Ph-a Sc-1	2.23	1.56	0.0	2.21	1.55	0.0	12.1	0
Ph-b Sc-1	2.15	1.50	0.0	2.15	1.50	0.0	12.1	120.3
Ph-c Sc-1	2.26	1.58	0.0	2.29	1.61	0.1	12.1	-119.3
Ph-a Sc-2	2.36	1.65	0.0	2.34	1.64	0.0	12.2	-0.1
Ph-b Sc-2	2.06	1.44	0.0	2.08	1.46	0.0	12.2	-115.3
Ph-c Sc-2	2.10	1.47	0.0	2.09	1.47	0.1	12.2	118.3
Ph-a Sc-1	2.18	1.52	0.0	2.15	1.51	0.0	24.1	0
Ph-b Sc-1	2.09	1.46	0.0	2.08	1.46	0.0	24.1	119.7
Ph-c Sc-1	2.24	1.57	0.0	2.25	1.58	0.1	24.1	-124.8
Ph-a Sc-2	2.29	1.60	0.0	2.27	1.59	0.0	24.3	0.0
Ph-b Sc-2	2.05	1.44	0.0	2.06	1.44	0.0	24.3	-111.0
Ph-c Sc-2	2.06	1.44	0.0	2.05	1.43	0.1	24.3	125.2
Ph-a Sc-1	2.21	1.55	0.0	2.17	1.52	0.0	48.4	0
Ph-b Sc-1	2.12	1.49	0.0	2.13	1.49	0.0	48.4	119.3
Ph-c Sc-1	2.28	1.60	0.0	2.29	1.60	0.1	48.4	-118.0
Ph-a Sc-2	2.29	1.61	0.0	2.27	1.59	0.0	48.5	0.90
Ph-b Sc-2	2.11	1.48	0.0	2.14	1.50	0.0	48.5	-113.5
Ph-c Sc-2	2.11	1.48	0.0	2.12	1.48	0.1	48.5	120.6
Ph-a Sc-1	2.16	1.51	0.0	2.14	1.50	0.0	96.1	0
Ph-b Sc-1	2.08	1.46	0.0	2.09	1.46	0.0	96.1	117.7
Ph-c Sc-1	2.22	1.56	0.0	2.23	1.56	0.1	96.1	-125.8
Ph-a Sc-2	2.30	1.61	0.0	2.28	1.60	0.0	96.8	-0.17
Ph-b Sc-2	2.03	1.42	0.0	2.04	1.43	0.0	96.8	-116.4
Ph-c Sc-2	2.05	1.44	0.0	2.06	1.44	0.1	96.8	123.6

Measurement of individual 30 turn coils

Induced voltage divided by magnetization speed ($n/60 \cdot 2\pi \cdot 2/N_p$) and the number of turns $N_t=12$, and the integration of the back emf at the highest test speed $n=50$ rpm.

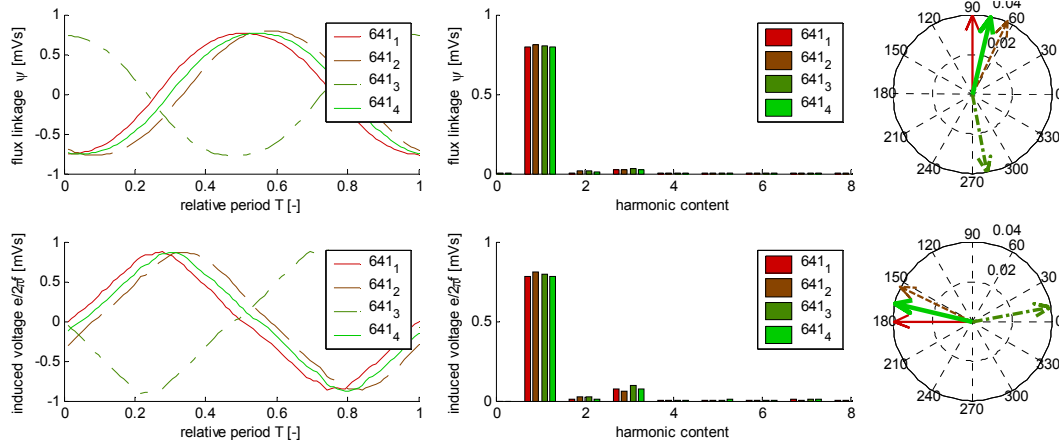


Figure 4.12 Voltage and flux linkage waveforms and phasors (ST2)

Table 4.9 Test results at selected speed and selected phase sections (ST2)

Test winding	Ψ_{m1} , [mVs]	Ψ_{rms} , [mVs]	Ψ_{THD} , [%]	E_{m1} , [mV]	E_{rms} , [mV]	E_{THD} , [%]	Freq, [Hz]	Shift, [deg]
Ph-a coil-1	0.79	0.56	0.0	0.78	0.55	0.0	4.2	0
Ph-a coil-2	0.81	0.57	0.0	0.81	0.57	0.0	4.2	-25.8
Ph-a coil-3	0.80	0.56	0.0	0.80	0.56	0.0	4.2	-169.4
Ph-a coil-4	0.79	0.56	0.1	0.79	0.55	1.1	4.2	13.3
Ph-a coil-1	0.80	0.56	0.0	0.79	0.56	0.0	12.0	0
Ph-a coil-2	0.82	0.58	0.0	0.82	0.58	0.0	12.0	-28.9
Ph-a coil-3	0.80	0.56	0.0	0.80	0.56	0.0	12.0	-168.9
Ph-a coil-4	0.80	0.56	0.1	0.80	0.56	1.0	12.0	13.4
Ph-a coil-1	0.78	0.55	0.0	0.77	0.54	0.0	12.1	0
Ph-a coil-2	0.81	0.57	0.0	0.81	0.57	0.0	12.1	-25.3
Ph-a coil-5	0.75	0.52	0.0	0.74	0.52	0.0	12.1	-158.8
Ph-a coil-4	0.79	0.55	0.1	0.78	0.55	0.9	12.1	-11.6
Ph-a coil-1	0.81	0.57	0.0	0.80	0.56	0.0	4.8	0
Ph-a coil-2	0.79	0.55	0.0	0.78	0.55	0.0	4.8	-36.1
Ph-a coil-5	0.83	0.58	0.0	0.82	0.58	0.0	4.8	-10.1
Ph-a coil-4	0.76	0.53	0.1	0.75	0.53	1.0	4.8	-22.9

Flux linkage as a function of rotation speed

The magnetic flux linkage is calculated as physical flux of the 5-coil phase segment. The flux linkage is calculated over the averaged values of a couple of periods. As the magnet placement is not identical and due to the eccentricity, there is additional variation between the measurements. Unfortunately, there is not enough measurement data in order to weigh the statistic thoughtfulness. However, there are accumulated data of two different measurements of the original magnet arrangement (left) and reconditioned magnet arrangement (right) for the same stator at different speeds and phase segments.

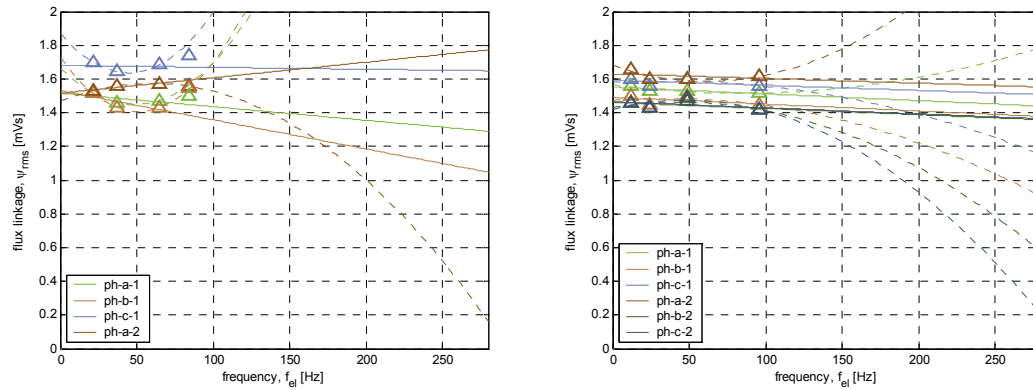


Figure 4.13 Flux linkage speed dependence investigation based on two sets of measurements (ST1)

Figure 4.13 on the left shows rms value of flux linkage of 4 phase segments as a function of electrical frequency. Triangular symbols indicate the measurement points, solid lines show the linear fit and dashed lines show the quadratic fit. The fourth measurement point confirms that the set of initial data is insufficient to draw a consistent conclusion. The trend of the flux linkage line as a function of speed, which is from zero-speed up to nominal speed, is expected to fall linearly -7.8% as an average of the four phase segments. The averaged flux linkage at zero-speed is 1.56 mVs.

Figure 4.13 on the right shows rms value of flux linkage of all 6 phase segments as a function of electrical frequency. Triangular symbols indicate the measurement points, solid lines show the linear fit and dashed lines show the quadratic fit. The trend of the flux linkage line as a function of speed, which is from zero-speed up to nominal speed, is expected to fall linearly -6.4% as an average of the four phase segments. The averaged flux linkage at zero-speed is 1.53 mVs.

Comparison of stator core with and without inserts

There are two emf measurements done relating to the stator (ST2) with inserts. As the stator winding is a concentrated distributed winding the each coil has a phase shift of 12 electrical degrees. This phase shift causes a voltage difference and causes circulating currents in the windings. Furthermore, the difference between the winding and the core, if it exists, causes an additional induced voltage difference. The first measurement considers the parallel-coupled phase segments (on the left) and the second one is based on the individual open circuited coils in a single-phase segment (on the right).

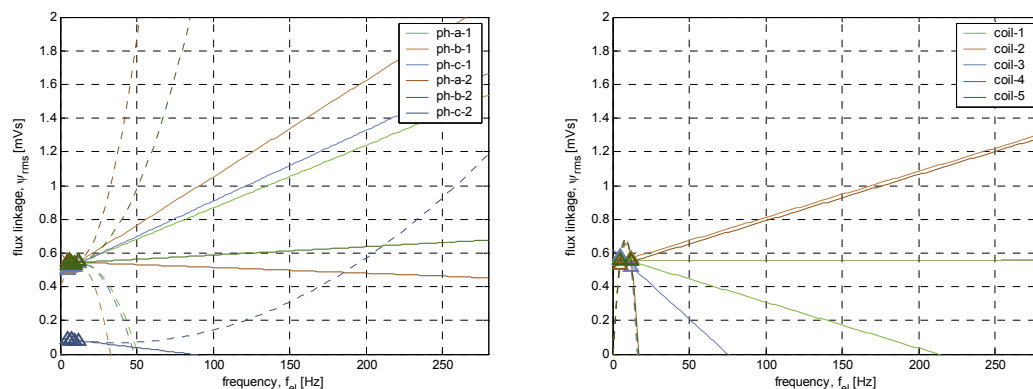


Figure 4.14 Flux linkage speed dependence investigation based on two sets of measurements (ST2)

There is impossible to say anything about flux linkage dependence on the speed.

When comparing the flux linkage of SM²C (BCVB050) core without inserts then one phase segment of five coils establish a linkage about 1.08 mVs while a single coil of a core with inserts can give 0.54 mVs in average near by “low speed”. By using a vector summation of distributed coils the expected flux linkage over a stator segment of series coupled coils comes up to 2.64 mVs i.e. factor of 1.7 compared to pure SM²C machine.

Induced rotor losses

Mechanical power losses and the magnetic power losses in the rotor are investigated with an IR camera after running the machines at different speeds (Fig. 10). The magnetic flux fluctuation is measured and modelled with a number of sensor coils around the magnet. It is very likely that the rotor yoke, which is made of solid material, suffers from eddy currents that cause losses, and is more visible the greater the magnetic permeability of the stator core.

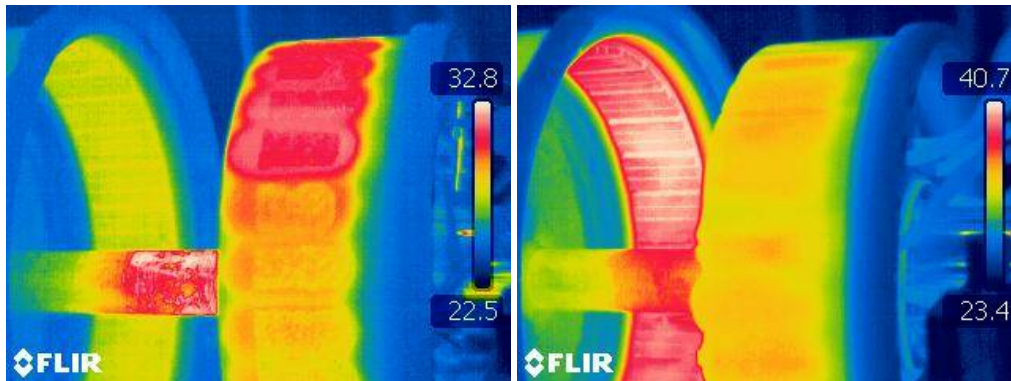


Figure 4.15 Temperature distribution over stator and rotor after 4 minutes run at 680 rpm for SM²C stator St1 and SMC insert stator St3. Different emissivity of the stator surface (on the left) may cause the misleading temperature readings.

4.4 Remarks for further development

There are some remarks that are stated here (after design and experimentation on W3 machines) concerning to further development:

1. Stator core: the main focus becomes on forming and compact winding with proper insulation. Anyway, if the winding production can take advantage of magnetic inserts, then it is forth to have it for a increased torque capability for an electrical machine,
2. Stator production – molding: If the winding production, assembling and molding can be with the same frame (or mold) it is forth considering it, importance relies on backing process that result homogeneous distribution of SM²C,
3. Winding: There is a range of wires that are most manageable to “soft deform” them into a coil. By considering the slot area and coil arrangement the different diameter of wire and allowed space, which is 1% of diameter, between them fills the area differently. It depends also how the corresponding layers are shifted and packed (especially when using bundles of parallel strands) (Figure 4.5),
4. Winding turns and coil turns: Concentrated windings are more manageable with high number of turns, which means usually lower application speed or higher terminal voltage by comparing 12 turns section and 5x30 turns section for wind turbine application (Figure 4.16). In this example: $n=200$ rpm results 46.6 Hz and 12 turn section parameters are 0.03 Ohm, 0.103 mH, $E_o=0.025$ and 0.04 Vs, which is respectively with and without inserts. (The single phase section is recalculated according to 300 turns that gives 12.5 times higher voltage, and 156 times higher voltage and resistance.).

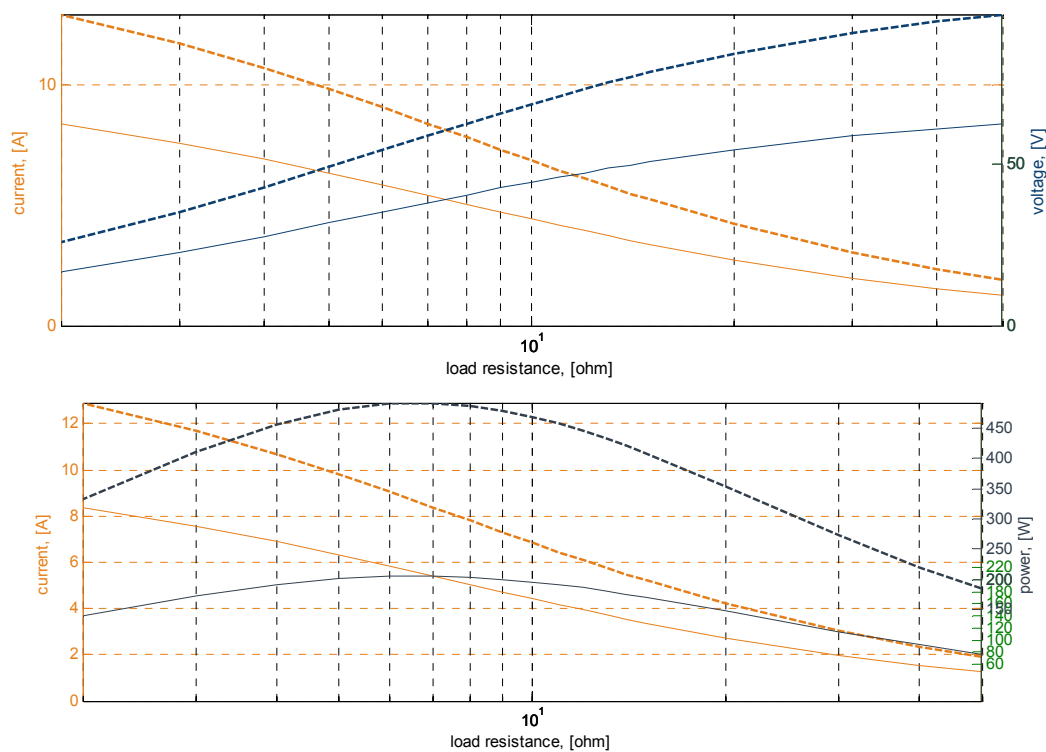


Figure 4.16 Load characteristics of ST3 at 200 rpm when using it for In-Wind application

The dashed lines of voltage, current and power indicate the characteristics of a ST3 stator at 200 rpm and the solid lines for ST2. The characteristics are per winding segment of 300 turns based on ST2 winding up-scaling, which means that the insert induction can be slightly larger due to higher permeability of the core. However, these results indicate that the machine with 30 turns per coil (ST3) can be attractive for wind power application. The coil can have even more turns if the higher voltage per phase and rotation speed is specified.

Production of dimensionally stable coils

Forming coils and fixating their dimensions prior to molding and mold design is one clear consequence of using SM²C core and winding design and production goes hand-in-hand. A concept visualization related to a [double-layer modular wave-winding](#) for machine design [1] and manufacturing in Table 1.1 is presented on as following:

1. Coil distribution in slot concerning to double-layer modular wave-winding and distributed concentrated winding (Figure 4.17),
2. A double-layer modular wave-winding for 28P30S Ø240/310 machine (Figure 4.18),
3. Parameterization of a double-layer modular wave-winding segment (Figure 4.19),
4. Double-layer modular wave-winding segments with tooth-tip formation ring (Figure 4.20),
5. Visualization of using mold to define fixation of components and tooth-tip (Figure 4.21),
6. Visualization of SM²C core when coils and mold is removed (Figure 4.22). Note there are two different approaches defining stator tooth tip here.

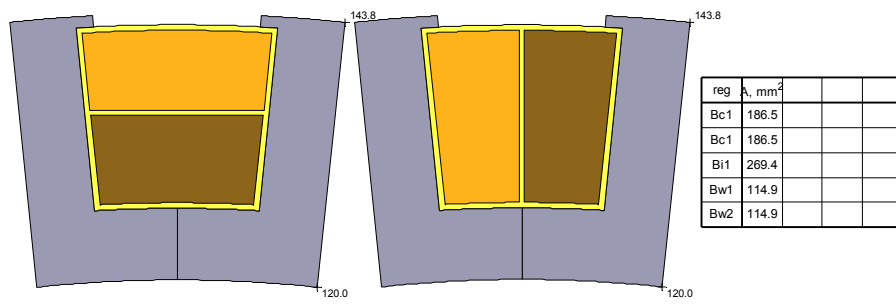


Figure 4.17 Coil distribution in slot for W3 design concerning to double-layer modular wave-winding and distributed concentrated winding

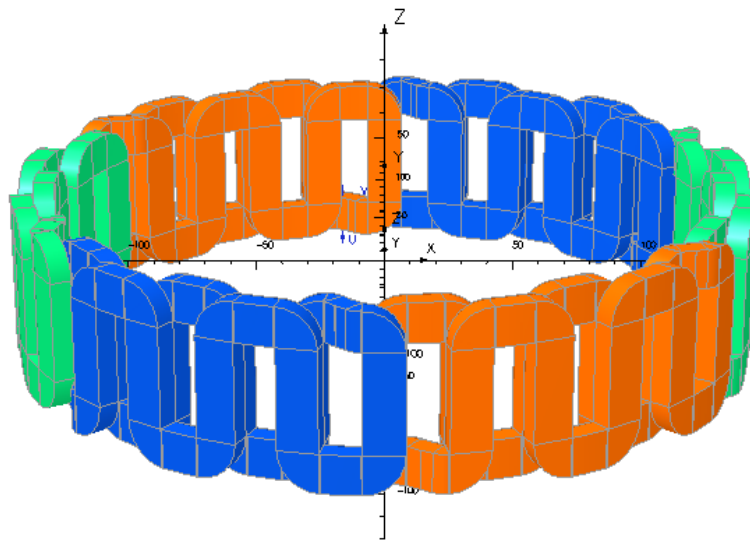


Figure 4.18 A double-layer modular wave-winding for 28P30S Ø240/310 machine

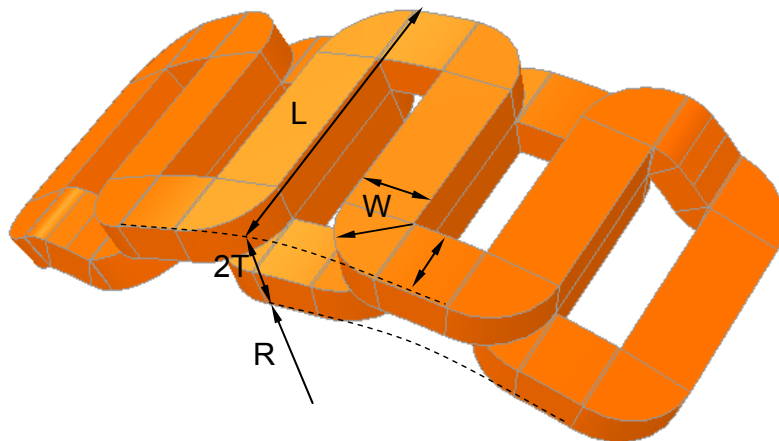


Figure 4.19 Double-layer modular wave-winding segment parameterization

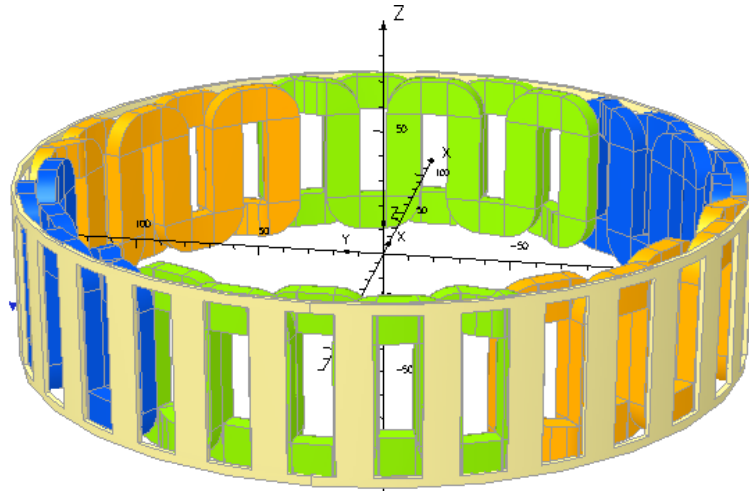


Figure 4.20 Double-layer modular wave-winding segments with tooth-tip formation ring

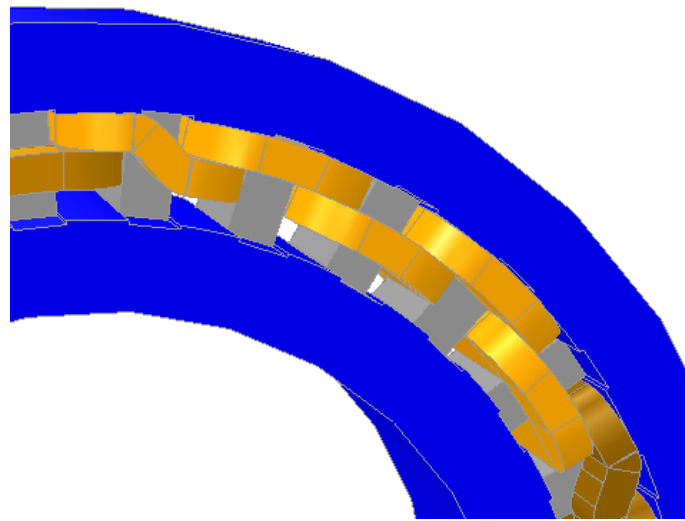


Figure 4.21 Double-layer modular wave-winding segments with inserts and mold form that includes tooth tip formation and fixation of inserts

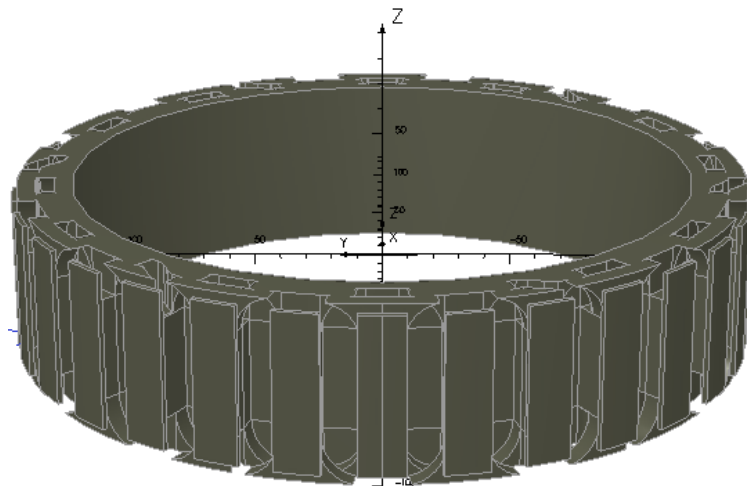


Figure 4.22 SM2C stator core as a subtraction of mold volume and windings with tooth-tip formation ring (Figure 4.20)

In this example, the coils are dimensioned (Figure 4.19) in accordance with the outer radius of the stator so that the top of the teeth is just defined by the coil opening. Alternatively, the windings are embedded into the core so that there is a small space (thickness of 2 mm) between the winding and the outer radius of the winding where the teeth can be formed so that the magnetic material covers the outer radius of the windings.

0 mm thickness for tooth-tip formation: Inner radius of the winding (R) is 126.4 mm. The thickness of the winding layer (T) is 8.3 mm, which gives the total thickness of the winding 16.6 mm, the middle radius 134.7 mm and the outer radius 143.0 mm. The width of the winding (W) is 14.8 mm, which is considered to be the bending radius of the winding if the inner radius is taken equal to zero. Length of the winding (L) is 67.5 mm.

2 mm thickness for tooth-tip formation: Inner radius of the winding (R) is 126.4 mm. The thickness of the winding layer (T) is 7.3 mm, which gives the total thickness of the winding 16.6 mm, the middle radius 133.7 mm, and the outer radius 141.0 mm. The width of the winding (W) is 14.8 mm, which is considered to be the bending radius of the winding if the inner radius is taken equal to zero. Length of the winding (L) is 67.5 mm.

5 Prototyping and evaluation of a small Ø190 PMSM

To produce moldable cores, it is important that all the necessary integrated components, such as the coil, are placed in the mold. During the development of the design and production of the coil in the project, investigators has come to a solution where the coil is made from a sheet of electrical conductor such as aluminum or copper and it is shaped so that openings are left between the turns of the material through which the cooling medium is passed [5][11]. As a result, a direct-cooled winding, or a laminated winding, named after the shape and manufacturing method of the conductor, is produced. Therefore, this machine did not need SM²C core rather than direct cooled winding to make the machine preferably smaller and (more) powerful. Since the shape of the coil resembles waves, it is called a wave coil or wave winding in the following text.

Specification: Di=90 mm, Do=200 mm, H=67 mm, Udc=48 V, nmax=350 rpm (1600W)

5.1 Mechanical design

Simplicity of design and manufacturing time have a much higher priority than machine performance. The initial design (of W4), a concept visualization is shown in Figure 5.1

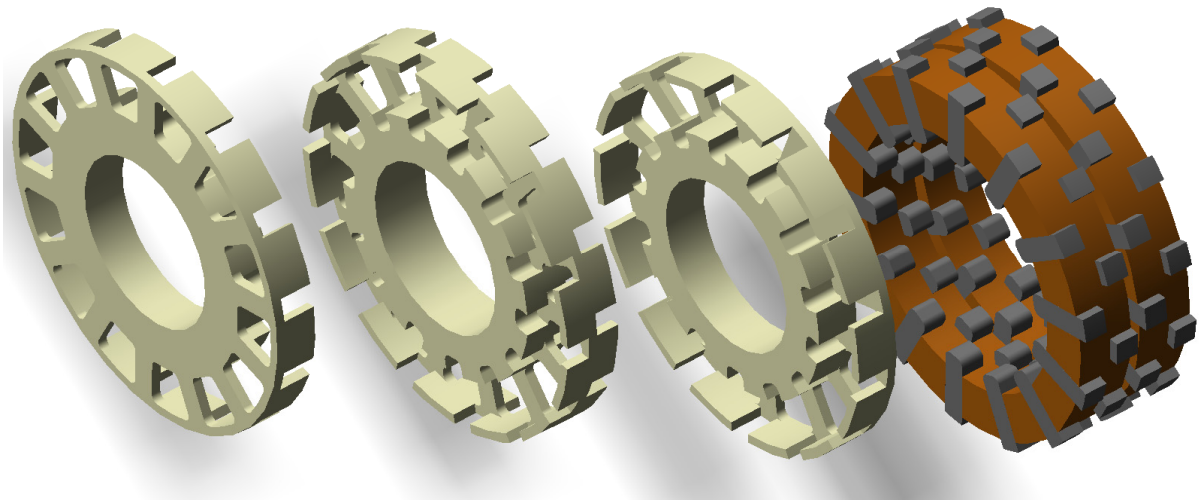


Figure 5.1 Initial design

Number of poles

Number of poles (N_p) is defined by the existing size of the magnets (5.0x8.5x60 mm) and the inner diameter of the outer rotor (180 mm). The theoretical maximum number of magnets is 60 (Figure 5.2). The selection criteria are: at least two magnets per pole (magnetic leakage) and at most two magnets per pole (magnetic measurement of rotor core) maximum number of poles $N_p=30$.

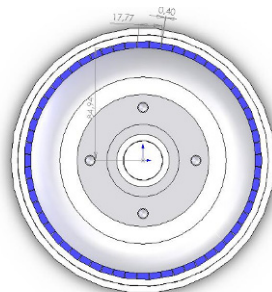
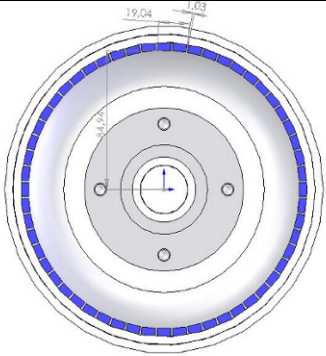
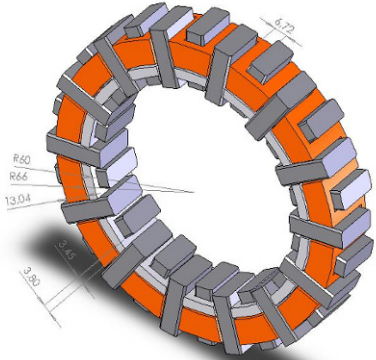
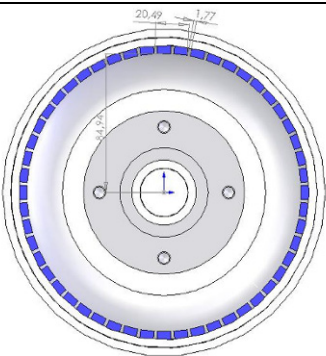
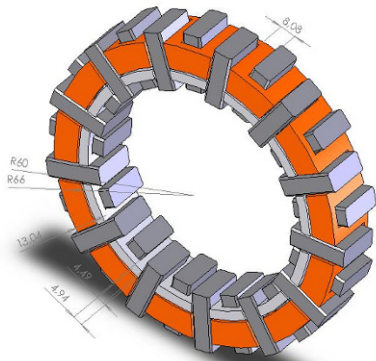
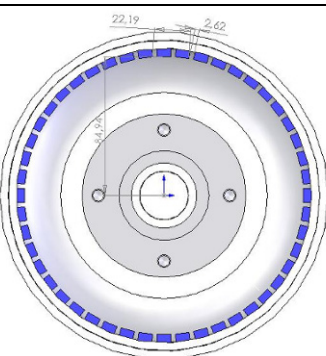
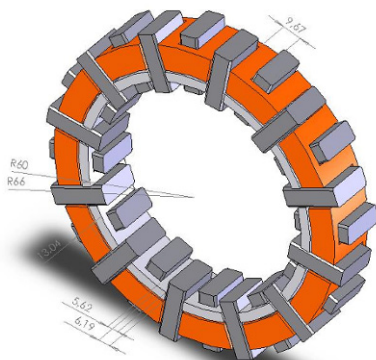
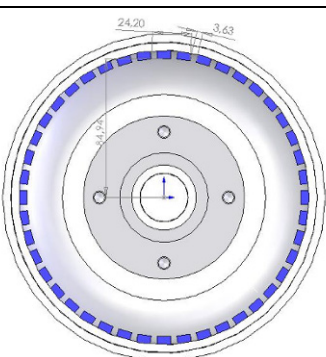
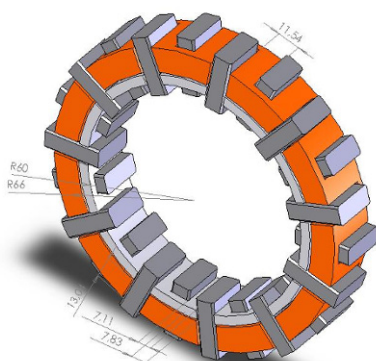


Figure 5.2 Placement of existing magnets as many as fits"

Optimum number of poles from the manufacturing point of view

The number of poles of electric machine defines excitation strength as well as dimensions of machine parts (Table 5.1).

Table 5.1 The selection of number of magnets and the impact to stator design

Np	Rotor	Stator segment
28	 <p>Technical drawing of a rotor cross-section for 28 poles. Dimensions shown: 19.04, 1.63, 44.24.</p>	 <p>3D perspective view of a stator segment for 28 poles. Dimensions shown: 6.27, R60, R66, 13.04, 3.80, 2.45.</p>
26	 <p>Technical drawing of a rotor cross-section for 26 poles. Dimensions shown: 20.49, 1.77, 44.24.</p>	 <p>3D perspective view of a stator segment for 26 poles. Dimensions shown: 8.08, R60, R66, 13.04, 4.47, 4.94.</p>
24	 <p>Technical drawing of a rotor cross-section for 24 poles. Dimensions shown: 22.19, 2.62, 44.24.</p>	 <p>3D perspective view of a stator segment for 24 poles. Dimensions shown: 9.82, R60, R66, 13.04, 5.62, 6.19.</p>
22	 <p>Technical drawing of a rotor cross-section for 22 poles. Dimensions shown: 24.20, 3.63, 44.24.</p>	 <p>3D perspective view of a stator segment for 22 poles. Dimensions shown: 11.54, R60, R66, 13.04, 7.11, 7.83.</p>

Compressed powder composite block (10x30x120) is the basis of stator construction with SMC teeth. The active length of the machine is connected to the magnet length (60 mm) and with two-phase machine with axial distance (4 mm) between the stator segments (28 mm), dimensions for an SMC tooth are 10x30x24 which would facilitate the manufacture. The following dimensions for a stator segment are selected (Table 5.2):

Table 5.2 The dimensions describing the size of stator parts

Stator component	Inner radius	Outer radius	Axial height
Stator teeth	$r_{si}=54.23$ mm	$r_{so}=48.15$ mm	$h_s=24$ mm
Stator yoke	$r_{yi}=60$ mm	$r_{yo}=65$ mm	$h_s=28$ mm
Wave winding	$r_{wi}=66$ mm	$r_{wo}=79$ mm	$h_w=27$ mm

Manufacturing vs assembly concept selections

Two alternative options for stator construction are discussed: 1) multi-set stators that are built up with load-bearing ends/parts, made of plastic and 2) individual stator segments that are attached axially to the machine end. Regardless of the choice, the realization solutions for stator yoke addressed: 1) stator yoke that follows the design of the wave winding, 2) stator yoke with enclosed cavity or punch hole, 3) material selection.

The image below (Figure 5.3) shows the stator construction of the stator segments where the segments consist of two identical assembly rings that define the placement of the SMC teeth and the rotation of the segments. Bandage over the SMC tooth tips is discussed to counteract normal forces between magnets and stator teeth.

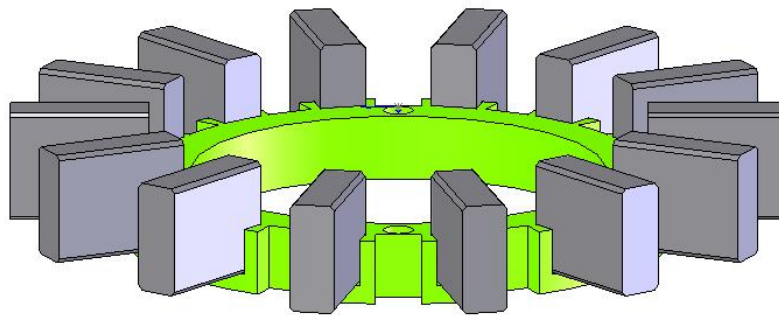


Figure 5.3 Attachment option for stator teeth

In the ideation phase, there are a number of constructive discussions, which unfortunately is not reported here.

5.2 Electromagnetic design

The main challenge of electromagnetic design is not only the consequences of normal forces on the stator teeth, but also tangential forces, which result in the expected high torque ripple and cogging. Similar to transversal flux machines, the number of magnets and stator teeth is exactly the same.

2D FE simulation of a phase segment

Calculation model is based on a sector of a phase segment where torque as a function of rotor position and stator current is calculated. Figure 5.4 shows driving torque over the total (Ampere turns) rms current in a phase winding (orange line with circle marking). The total current is the sum of the current in all winding turns. The figure also shows the relative torque ripple over drive torque (blue-grey line with rectangle marking).

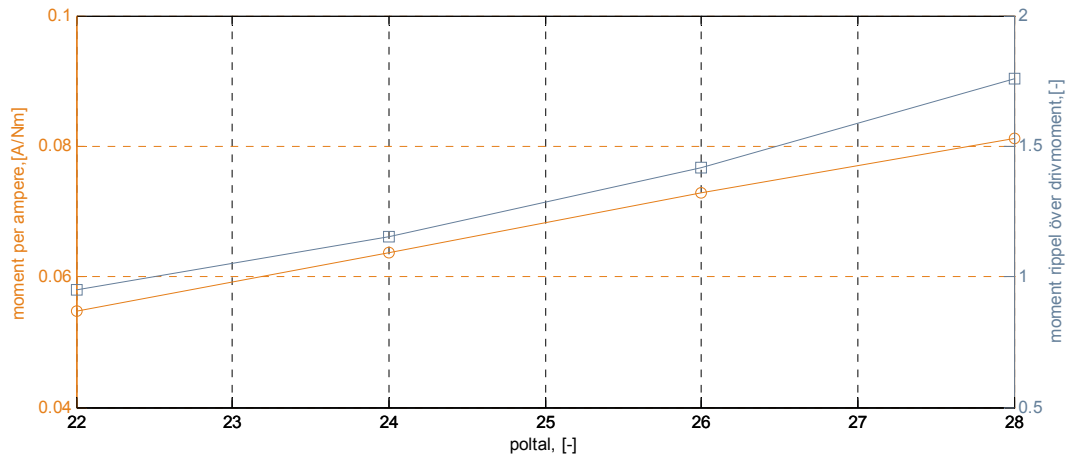


Figure 5.4 Torque and ripple as a function of number of poles

Geometry data of a 28-pole phase segment is shown in Figure 5.5

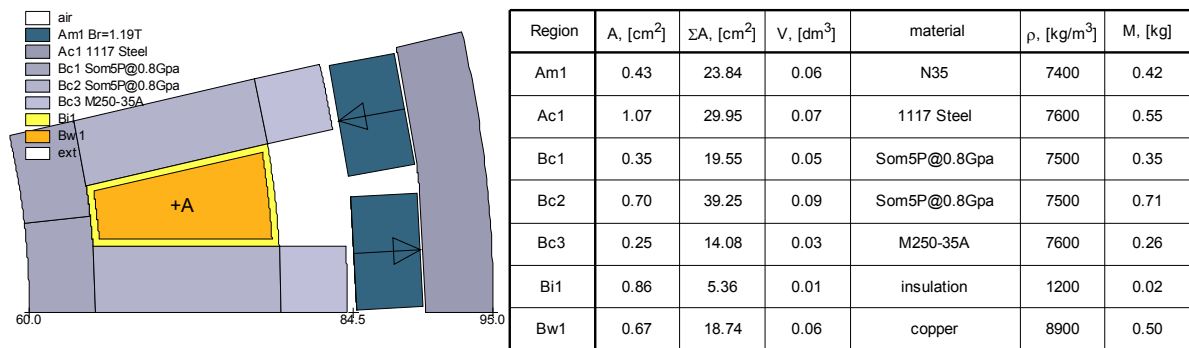


Figure 5.5 28-pole machine geometry presentation in slot level

Insulation thickness between stator winding and parts of magnetic core is 0.5 mm. Conductor area is chosen 60% less than winding area and with 10 A/mm² current density the total current of a 28-pole machine is 402 A. The magnitude of the current and the load angle are chosen from current component vectors: $is_x = \{-1 \ -2/3 \ -1/3 \ 0\} \times 10 \text{ A/mm}^2$ and $is_y = \{0 \ 1/3 \ 2/3 \ 1\} \times 10 \text{ A/mm}^2$. The color codes for the torque curves are shown in Figure 5.6 Color presentation of current vector magnitude and load angle used in Table 5.3.

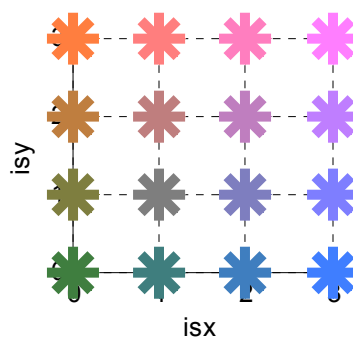
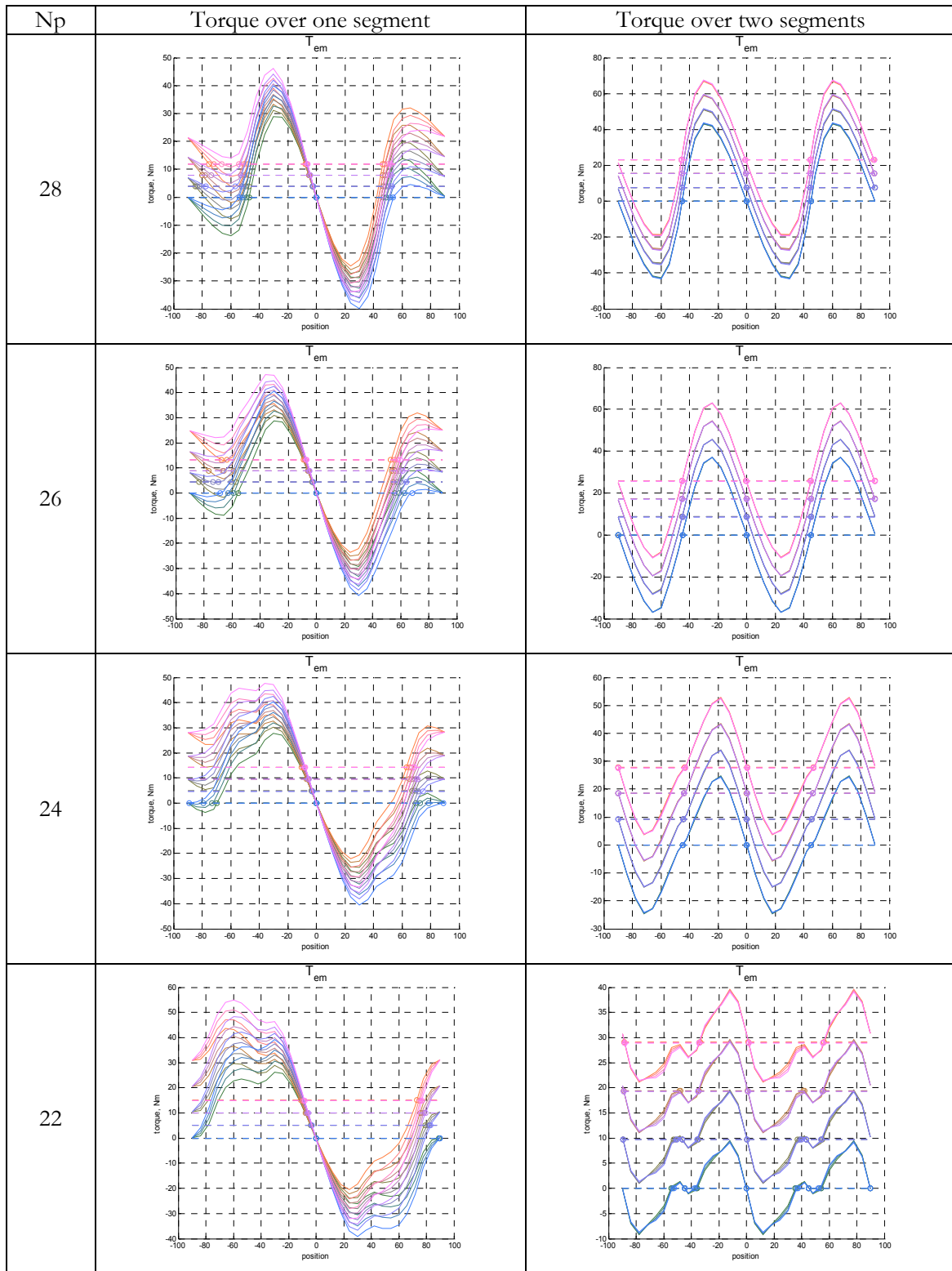


Figure 5.6 Color presentation of current vector magnitude and load angle used in Table 5.3

The following Table 5.3 shows static torque characteristics over one phase segment and pole, as well as over two angularly displaced phase segments and pole.

Table 5.3 Torque as a function of current and rotor angle for a single and two segment arrangement



Summary of torque capability vs quality is shown in Table 5.4 where J shows current density in A/mm².

Table 5.4 Comparison of machine parameters as a function of number of poles and current density

Np	f [Hz]	Total current [A]			Electromagnetic torque [Nm]			Torque ripple [Nm]			Relative torque ripple [%]		
		J=3.3	J=6.6	J=10	J=3.3	J=6.6	J=10	J=3.3	J=6.6	J=10	J=3.3	J=6.6	J=10
28	82	134	268	402	7.70	15.4	23.1	86.9	86.9	86.9	1129	565	376
26	76	166	332	499	8.63	17.1	25.7	73.9	73.8	73.8	856	430	287
24	70	204	408	612	9.24	18.4	27.6	48.5	48.4	48.3	525	262	175
22	64	248	497	745	9.66	19.2	28.8	17.8	17.7	17.6	184	92.1	61.1

The electromagnetic effect over two phase segments (200 rpm), and the power losses in one phase segment (350 rpm) are shown in Table 5.5. Conductor losses are shown over the active part (24 mm in z-direction) of wave winding.

Table 5.5 Comparison of machine parameters as a function of number of poles and current density

Np	f [Hz]	Power loss in stator one coil [W/l]			Electromagnetic power @ 200rpm [W]			Power loss density in stator core [W/l]			Power loss in stator one core [W]		
		J=3.3	J=6.6	J=10	J=3.3	J=6.6	J=10	T _{top}	T _{tand}	Rygg	T _{top}	T _{tand}	Rygg
28	82	6.0	24.0	54.0	161	322	483	30.0	70.7	20.4	1.41	6.66	0.69
26	76	6.9	27.6	62.1	180	358	538	29.8	66.6	19.0	1.40	5.82	0.68
24	70	7.8	31.3	70.5	193	385	578	28.9	61.3	17.4	1.36	4.95	0.50
22	64	8.7	34.9	78.6	202	402	603	27.3	54.6	15.4	1.28	4.04	0.41

Magnet arrangement and cogging

The best regular arrangement of 22-pole magnet system is selected for 2-phase 22-tooth stator segment. For the sake of continuation towards 3-phase low cogging machines 24-tooth and 21-tooth arrangements are under development. Two different magnet arrangement, torque per segment and over two segments are shown in Figure 5.7.

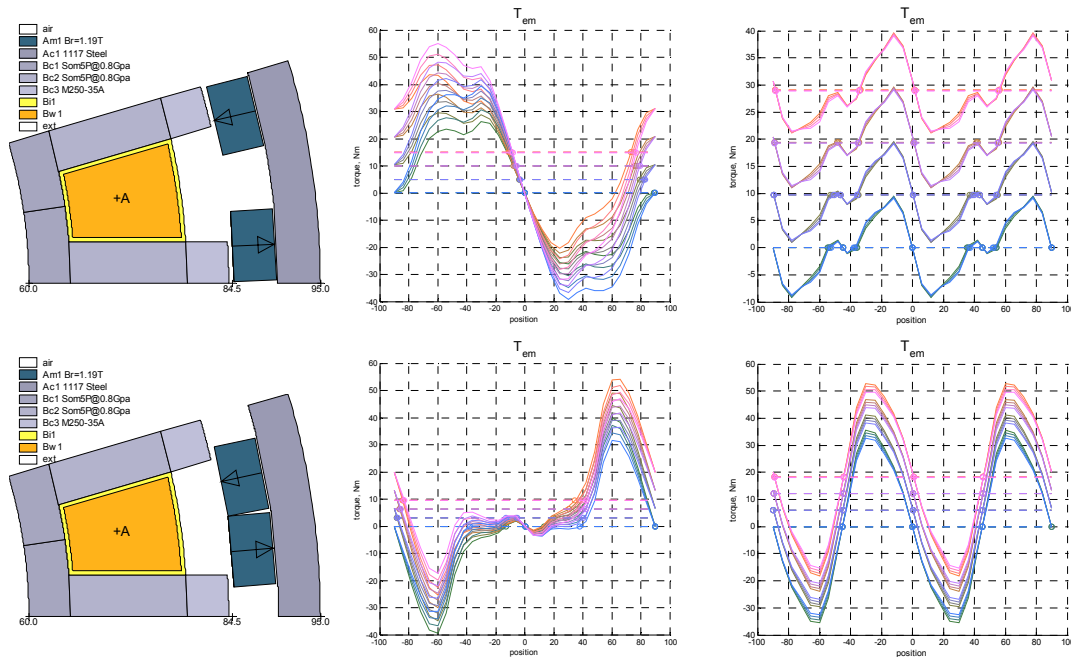


Figure 5.7 Slot visualization and magnet arrangement for 22-pole machine and corresponding static torque curves

There are two extremes of evenly distributing and placing two-magnets per pole: a) poles connected (e.g. NN-PP-NN-...) (Figure 5.7 top) or b) poles detached (e.g. NP-PN-NP-...) (Figure 5.7 bottom). Magnet arrangements with the poles-connected (PC) gives less leaky fundamental magnetization and puts more stress on adhesive mounting (glue) of surface mounted permanent magnets. Alternatively, the poles-detached (PD) arrangement gives leaky magnetization with higher space harmonic content, but at the same time mechanically more stable system that can sustain high load force and torque. However, there is a noticeable difference in magnetic loading in the core, flux density distribution in the air gap and flux linkage (Figure 5.8).

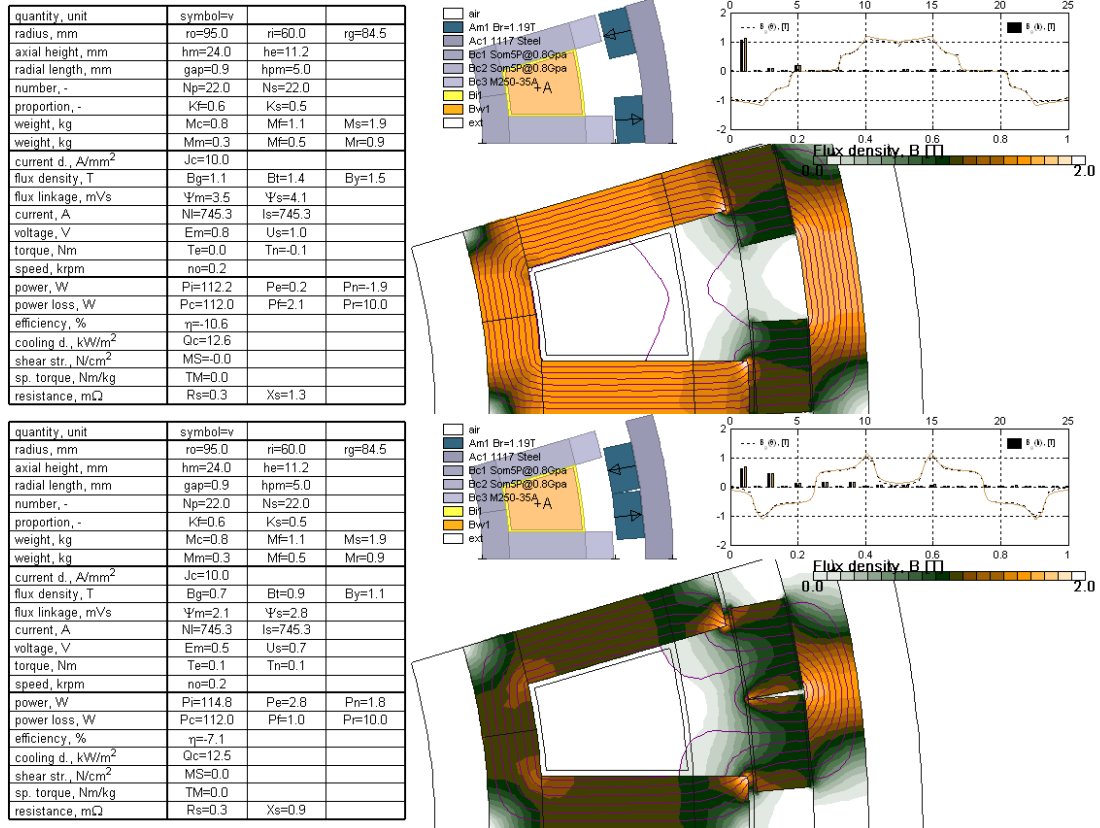


Figure 5.8 Flux density and flux linkage estimation depending on magnet arrangement and placement

There are two main aspects on magnet arrangement and fixation:

- Arrange the tangential magnetic forces so that the cogging is reduced with the least loss of the driving torque,
- Reduce mechanical loadings in the PM assembly as the adhesive contact between the planar and the cylindrical surface is small but stressed by magnetic forces between the magnets and machine parts.

5.3 Prototyping and evaluation process

The design for prototyping is shown in Figure 5.9 and the evaluation steps in Figure 5.10.

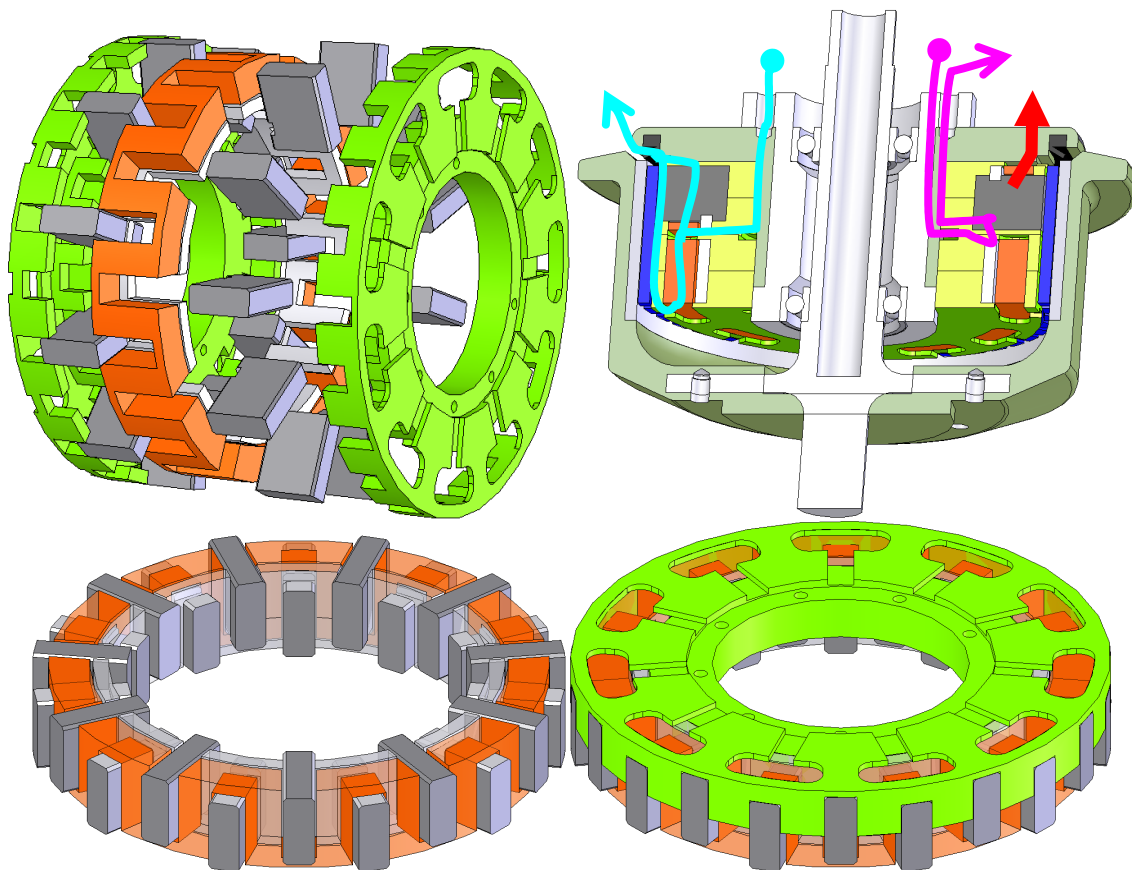


Figure 5.9 Explode view of a stator segment and cross-section view of the assembled machine including the electric and cooling paths (above) and stator segment mounting (below)

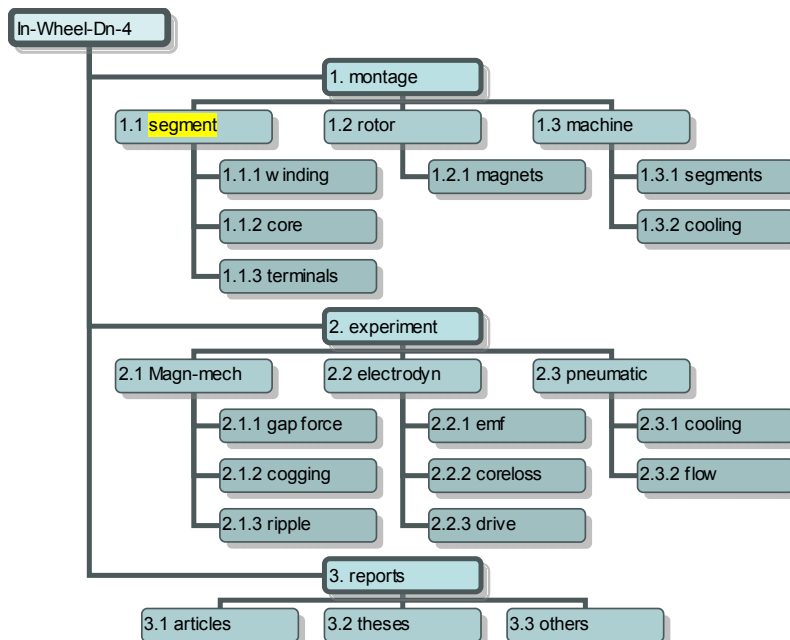


Figure 5.10 Evaluation steps and reporting

Laminated wave winding

The laminated wave winding (Figure 5.11) is produced according to the information provided in [5][11] and that also for electric insulation system between the turns. Importance of the cutting process precision is important, as when the strip of the foil coil is rolled up as a wave, the slots of the winding should come into a fine alignment.

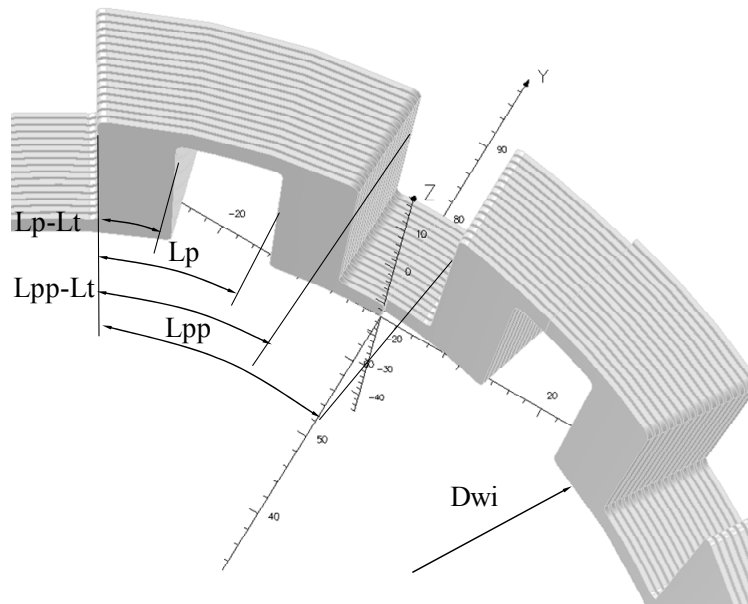


Figure 5.11 Parameterized geometry of laminated wave winding

Evaluating while assembling

The assembling process facilitates analysis of the machine while mounting. An example is given on mounting the permanent magnets as pairs on the inner surface of the rotor core (Figure 5.12). Since the magnets are “glued” by the magnetic forces the induced voltage (Figure 5.12) and cogging torque (Table 5.6) measurements could be performed.

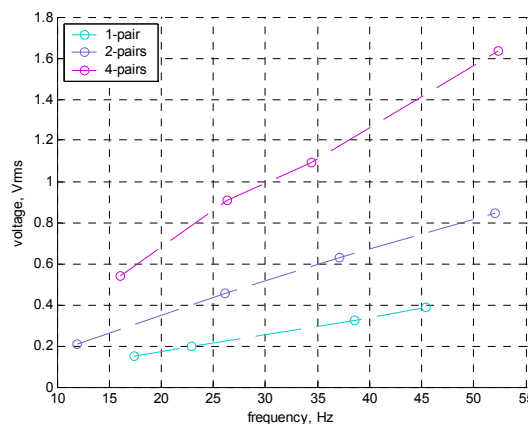


Figure 5.12 4-pairs of detached-pole placed permanent magnets (10-FEB-2013)

The peak cogging is approximately detected over the outer radius of rotor (Rro=101mm) and with PD-magnet arrangements for 1, 2 and 4 pairs of magnets.

Table 5.6 Cogging measurements with partial PM arrangement

Magnet pairs	1 (kg/Nm)		2 (kg/Nm)		4 (kg/Nm)		22-pole
Segment-1 (solid)	1.0-2.0	1.5	2.5-3.5	3.0	6.5-7.5	6.9	38 Nm
Segment-2 (laminated)							

The estimation of cogging per stator segment goes with the expected peak values for cogging. The second phase segment is not measured due to constructional problems.

The RLE parameters for the windings are estimated from the calculations. The inductance varies with current loading and the value here presents light loading.

- Calculated inductance of 22-pole 17-turn wave-winding: 0.268 mH (M250-35A yoke),
- Calculated flux linkage of PD-magnet arrangement: 35.9 mVs,
- Calculated flux linkage of PD-magnet arrangement: 59.9 mVs.

Calculated resistance of 22-pole 17-turn wave winding made of aluminum: $R=0.176$ Ohm obtained from $2.8e-8 (2\pi \cdot 72e-3 / (3.5e-3 \cdot 0.5e-3) + 22 \cdot 24e-3 / (9.5e-3 \cdot 0.5e-3)) \cdot 17$

Assembling / Re-assembling

The block magnets are glued on the solid rotor back iron and the assembling of stator segments is the concern since there are number of criteria to be full filled. The slot liner, which is mounted on stator teeth needs to survive the assembling process when a single tooth is moved into winding slot and after the stator is assembled into the machine where the normal forces appear. The process of re-insulating provides extra insulation on the stator teeth and reduces the risk of damaging the insulation, also reducing the risk of coolant leak between the teeth and the winding. From cooling perspective, a radial equal spacing between the winding turns is important, as high coolant velocity between every layer is vital. The stator core has also a sensing coil, which can be seen among the stator parts in Figure 5.13.

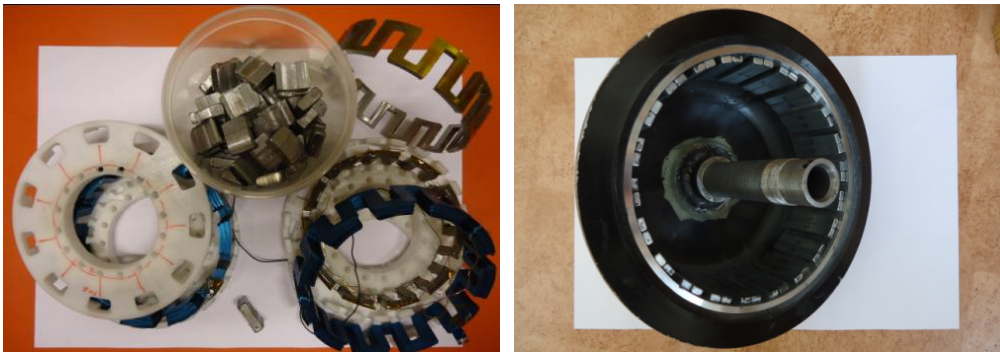


Figure 5.13 Stator parts (left) and assembled rotor (right)(17-JUN-2013)

There are a few attempts on reassembling the stator segments and these are due to insulation fault when placing the plastic holders tighter and another fault has been related to the magnetic forces in the air gap. The half-assembled stator segments are shown in Figure 5.14.

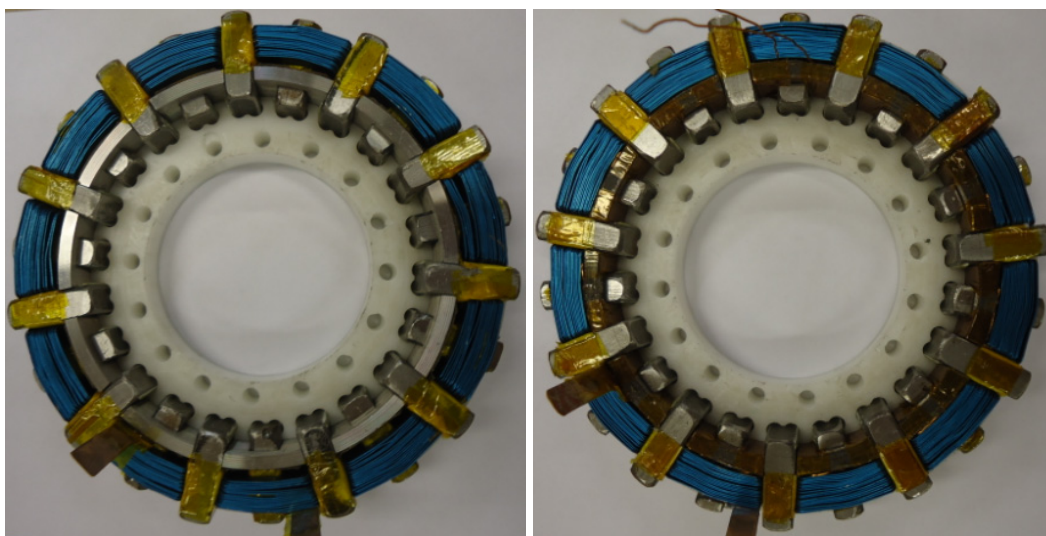


Figure 5.14 Half-assembled stator segments with solid stator yoke (left) and laminated stator yoke (right)

Winding parameters

Winding parameters are measured by using instruments (Table 5.7) and HAMEG RLC tester and this is done as a part of stator segment completion testing. Figure 5.15 shows winding parameters and the change in measurement results and some inconsistency of measurements that request deeper investigation for the sake of assembling quality inspection and machine performance evaluation (as the measurements are carried out at different time instances with changes in assemblies).

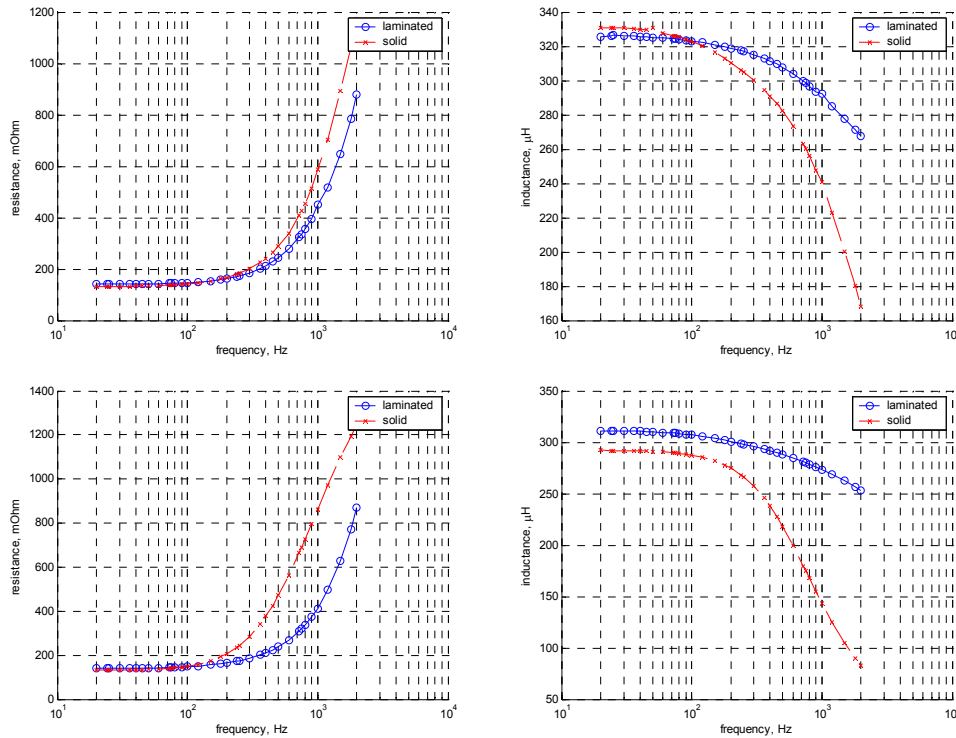


Figure 5.15 Winding parameters after two following assembling processes.

Table 5.7 An handheld instrument based RLC measurements

Agilent U1731A	R (120Hz/1kHz)		L (120Hz/1kHz)		C (120Hz/1kHz)		Ro
Segment-1 (solid)	0.377Ω	0.912Ω	248μH	49.5μH	3.10mF	74.9μF	34m/32m
Segment-2 (laminated)	0.153Ω	0.184Ω	50μH	3.0μH	2.36mF	116μF	

Peak Tech	R (120Hz/1kHz)		L (120Hz/1kHz)		C (120Hz/1kHz)		Ro
Segment-1 (solid)	0.235Ω	0.794Ω	250μH	52.1μH	2.73mF	70.5μF	38m/36m
Segment-2 (laminated)	0.158Ω	0.912Ω	55μH	4.2μH			

Escort ELC-133A	R (120Hz/1kHz)		L (120Hz/1kHz)		C (120Hz/1kHz)		Ro
Segment-1 (solid)	0.397Ω	1.009Ω	252μH	59.1μH		71.2μF	34m/32m
Segment-2 (laminated)	0.206Ω	0.240Ω	52μH	4.4μH			

No-load voltage

Figure 5.16 shows induced voltages over main winding and sensor coils of segment with solid yoke (left) and the other segment with laminated yoke (right). The measurements are taken from different time instances and represent different outcomes of machine assembly (Figure 5.12).

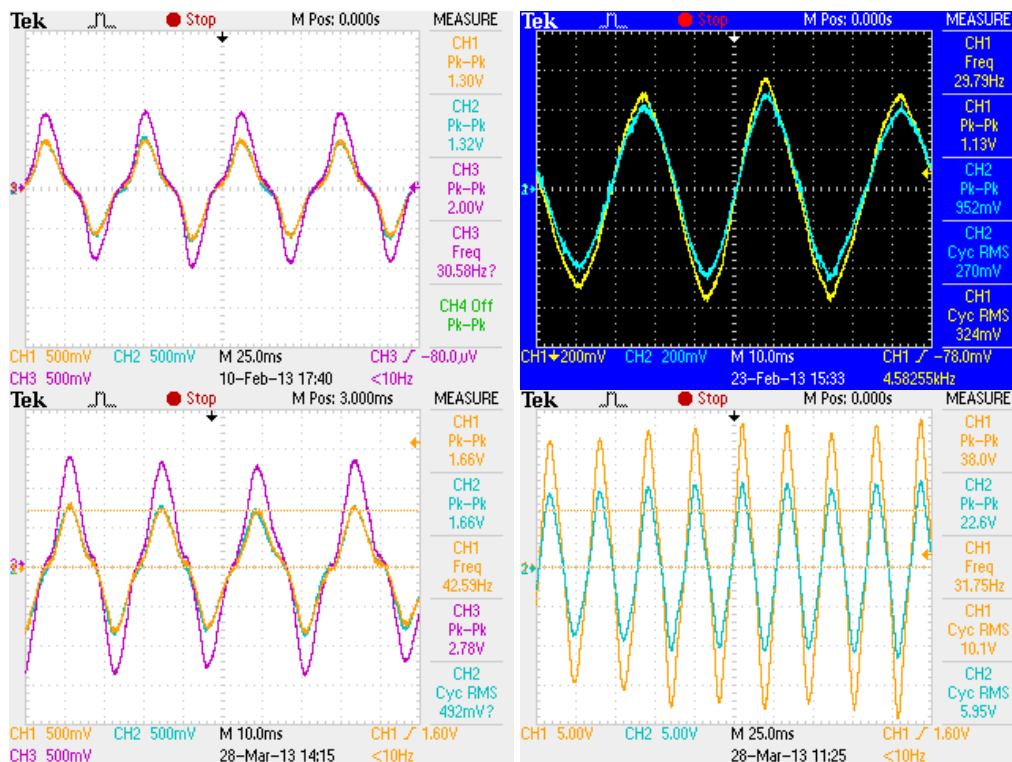


Figure 5.16 No load voltage measurements of the phase coils and the pick-up coils

Image on the Figure 5.16 shows emf measurement of the 1st phase segment with solid stator yoke (CH3 is the main winding) and the figure on the left shows the measurement for the second phase segment with the laminated stator yoke (CH1 is the main winding). The sensor signals are amplified by factor of 10 in order to make measurements comparable, but surprisingly the difference is not by factor of 1.7!

The **back-emf measurements** show that poles detached (PD) arrangement of view pairs of magnets give 8.5mVs/Hz/pole, which is 29.8 mVs as flux linkage rms value over the complete magnetized core and 42.1 mVs in peak compared to 35.9 mVs from the 2D FEA.

There is a limited amount (just 3 attempts on this occasion on February 10) of emf measurements on the second stator segment. Unfortunately, these measurements indicate that the magnetic core has a lower ability to conduct magnetic flux. The measurements show 6.5mVs/Hz/pole, which is 22.7 mVs rms and 32.2 mVs peak of flux linkage.

The sensor pick-up coils show approximately the same value when looking at the radial placement of the coil, next to stator yoke or next to air-gap. A more interesting aspect of the analysis is the voltage difference between the single wave-winding with round wire and the laminated wave-winding that is not 17 times (number of turns) but less and considerably smaller for the second phase segment.

Forced Cooling of the Stator Segment

There channels for coolant distribution are included into the plastic holder and the desired coolant flow for the machine is shown in Figure 5.9. There is 2x6 mm angular cavity along the inner edge of the phase segment and 0.8x6 mm radial channels from the angular cavity to the winding opening intended to provide coolant distribution and supply inside the assembled machine. The evaluation of stator segment cooling is reported in [12].

Manufacturing-to-design interactions

The practical experimentation provides a considerable amount of feedback to the design where many of the issues are oversimplified or taken as granted. As an example, conductor distribution and spacing in Figure 5.11 and Figure 5.17 (left) as well as the precision of winding slot dimensions are different. The cabling and termination often get little attention in the design initialization and may complicate the rational practical realization. For the sake of this machine is the termination from aluminum to copper provides challenges when packing tight the machine components (Figure 5.17 right).

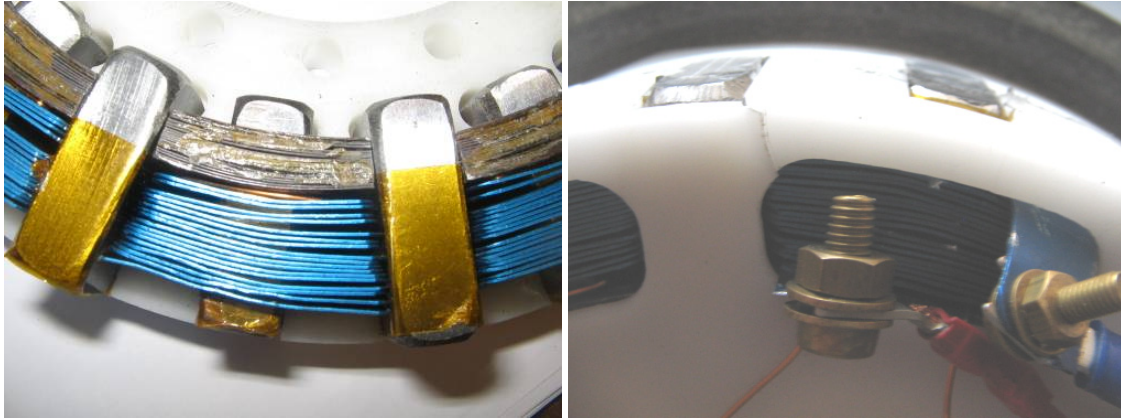


Figure 5.17 Detail view on the actual placement of the anodized conductor and teeth assembly (left) and the termination of the coil.

6 Conclusions and future work

The ultimate goals of this work in Damia-2 have reached a satisfactory end as the W3 machine SM²C with drive unit is completed and has been demonstrated in exposition and fair including a number of publications. The central goal of this work is achieved, as different ideas are evaluated based on 2D and 3D FE, experimentally evaluated and competence on design and manufacturing established. Unfortunately, the result of the work does not allow an outcome that could be put into production, but rather the experience and details necessary for development work.

1. 4 different machine designs have been thoroughly researched and two of them have been manufactured and tested incorporating different stator configurations (W3) or modifications (W4). Stator cores with rotomolded SM²C and SMC inserts are examined where the **crucial parameters** such as flux linkage and torque capability improvement are mainly examined.
2. The essential part of machine specification is related to **manufacturability for design**, where usually the simple arrangement for production does not establish a good design for electromechanical energy conversion. The originality of this (Damia-2) project is the reversed order for the electrical machine production, where the **windings** with insulation comes first and molding is used as an assembling process to compile the pieces into a mold into a single piece, brings up many new ideas, establishes a broad basis of design and manufacturing experience.
3. The choice of the topology of the stator winding with a **rational manufacturing** method that allows using the advantages of the SM²C material and molding.

References

References related and outcomes of the research

- [1] Reinap, A., Alaküla, M. (2012), "Impact of soft magnetic material on construction of radial flux electrical machines". *IEEE Transactions on Magnetics*, vol. 48, no. 4, pp. 1613-1616.
- [2] Högmark, C. (2008), "Making of a Torus Machine", *MSc Thesis, Lund University*, TEIE-5260,
- [3] Caesar T., Nilsson, S. (2010), "Utveckling av styrprogram till – samt provning av hjulmotor". *MSc Thesis, Lund University*, TEIE-5272,
- [4] Reinap, A., Hagstedt, D., Högmark, C., Alaküla, M. (2011), "Evaluation of a Semi Claw-Pole Machine with SM²C Core". *International Electrical Machines and Drives Conference (IEMDC2011)*, Niagara Falls, Ontario, Canada, May 15-18, 2011
- [5] Högmark, C., Reinap, A., Frogner, K., Alaküla, M. (2012), "Laminated winding with rapid cooling capability for electrical machines". *International Conference for Inductive and Electromagnetic Components, Systems and Devices including Manufacturing and Processing (INDUCTICA 2012)*, Berlin, Germany, June 26-28, 2012.
- [6] Reinap, A., Svensson, L., Alaküla, M., Andersson, M., (2012), "Design and evaluation of molded powder-core machine for in-wheel drive application". *International Conference on Electrical Machines (ICEM2012)*, Marseille, France, Sept. 2-5, 2012.
- [7] Svensson, L., Reinap, A., Andersson, M., Alaküla, M. (2012), "New manufacturing methods for electric motors using different soft magnetic material combinations". *International Electric Drives Production Conference and Exhibition (EDPC2012)*, Nuremberg, Germany, Oct. 16-17, 2012.
- [8] Svensson, L., Frogner, K., Reinap, A., Högmark, C., Andersson, M., Alaküla, M. (2012), "Alternative production process for electric machine windings". *International Electric Drives Production Conference and Exhibition (EDPC2012)*, Nuremberg, Germany, Oct. 16-17, 2012.
- [9] Högmark, C., Andersson, R., Reinap, A., Alaküla, M. (2012), "Electrical Machines with Laminated Winding for Hybrid Vehicle Applications". *International Electric Drives Production Conference and Exhibition (EDPC2012)*, Nuremberg, Germany, Oct. 16-17, 2012.
- [10] Andersson, R., Högmark, C., Reinap, A., Alaküla, M. (2012), "Modular Three-phase Machines with Laminated Winding for Hybrid Vehicle Applications". *International Electric Drives Production Conference and Exhibition (EDPC2012)*, Nuremberg, Germany, Oct. 16-17, 2012.
- [11] Conny Högmark (2013), "Moulded Electrical Machines and Laminated Windings", *Lic Thesis, Lund University*, TEIE-1066,
- [12] Kjellstrand R., Akujärvi V. (2013), "Modeling and evaluation of laminated windings". *MSc Thesis, Lund University*, TEIE-5311